MATERIALS CHEMISTRY FRONTIERS

CCS 中国化学会 CHINESE CHEMICAL SOCIETY

ICCAS

ROYAL SOCIETY OF CHEMISTRY

REVIEW

View Article Online
View Journal | View Issue

Cite this: *Mater. Chem. Front.*, 2023, **7**, 4420

Recent advances and prospects for organoboron-based thermally activated delayed fluorescence emitters

Liang Wan, Zhuang Cheng, Futong Liu and Ping Lu *

Received 1st May 2023,
Accepted 6th June 2023

DOI: 10.1039/d3qm00498h

rsc.li/frontiers-materials

The intense interest in organic boron-containing light-emitting materials stems from their attractive potential electron-deficient characteristics and excellent fluorescence efficiency. Delicate molecular design of organic boron-containing emitters and comprehensive studies of the relationship between their chemical structures and photophysical properties are of great significance for developing high-performance emitters. In this review, an overview of the recent studies on organoboron-based emitters for applications in organic light-emitting devices (OLEDs) is presented. First, we give a brief introduction to the basic properties of organoboron materials. And then, the recent research progress of thermally activated delayed fluorescence (TADF) materials containing triaryl/diarylboron, 10*H*-phenoxaborin, 5,9-dioxa-13*b*-boranaphtho[3,2,1-*de*]anthracene (DBNA), and 5,9-diphenyl-5,9-dihydroquinoxalino[3,2,1-*de*]phenazine (DABAN) is reviewed systematically with a focus on the molecular design, photophysical properties and performance of the corresponding OLEDs. Finally, the future challenges of organoboron-based materials are discussed.

1. Introduction

Boron (B) is the fifth element in the periodic table with an atomic mass of 10.81. It is a non-metallic element with the most electronegativity among elements of Group III. Boron is abundant in nature, mainly distributed in borax ($Na_2B_4O_7 \cdot 10H_2O$), priceite ($Ca_2B_6O_{11} \cdot 5H_2O$) and magnesite ($Mg_2B_2O_5$), among which borax was used as medicine in ancient times.[1] Boron chemistry has a long history. In 1702, French chemist Holmberg first heated borax and ferrous sulfate together to prepare boric acid.[2] In 1808, pure elemental boron was first isolated independently and simultaneously by H. Davy in England, who observed that electric current sent through a solution of borates produced a brown precipitate on one of the electrodes, and J. Gay-Lussac and L. Thenard in France obtained boron by reducing boric acid with iron at high temperature.[3] Organoboron chemistry has a profound influence on chemical research and industry, including synthetic chemistry, biochemistry, pharmaceutical chemistry, materials science, *etc.* In the past decades, it also has witnessed the rapid development of organic optoelectronic functional molecules.[4] The electron structure of boron is $1s^2 2s^2 2p^1$ with four valence orbitals and three valence electrons. Thus, sp^2 hybridized three-coordinate boron compounds can be formed with electron-deficient properties. They show high potential in nonlinear optics, chemical sensing, biological imaging, and especially, in the field of organic electroluminescence.[5,6]

In 1987, Tang and VanSlyke first reported the preparation of organic light-emitting diodes (OLEDs).[7] Since then, OLEDs have been actively studied owing to their advantages of low power consumption, high brightness, color purity, lightweight, large viewing angle and flexibility and have been commercially applied in some flat-panel display applications such as mobile phones and televisions.[8,9] According to spin statics, 25% singlet excitons (S_1) and 75% triplet excitons (T_1) are generated after hole and electron injection in OLEDs. Thermally activated delayed fluorescence (TADF) emitters emerged as new-generation luminescent materials to fabricate highly efficient OLEDs by enabling 100% IQE through reverse intersystem crossing (RISC) based on a tiny energy gap (ΔE_{ST}) between singlet and triplet states.[10] To achieve a small ΔE_{ST}, the most common way to design TADF molecules is to sufficiently separate the frontier molecular orbitals by appropriate selection of donor (D) and acceptor (A) units with different electron-donating and electron-accepting abilities.[11] Organoboron-based groups with an empty p-orbital and intrinsic electron-deficient nature can serve as suitable π-electron acceptors to construct TADF emitters with D–A and D–π–A structures. In such molecules, in order to protect the empty p-orbital from being attacked by nucleophiles and enhance the stability of the compound under ambient conditions, the boron atom is commonly linked with sterically bulky aryl groups, such as 2,4,6-trimethylphenyl

State Key Laboratory of Supramolecular Structure and Materials, Jilin University, Qianjin Street No. 2699, Changchun, 130012, P. R. China. E-mail: lup@jlu.edu.cn

and 2,4,6-triisopropylphenyl.[12–15] In 2016, Hatakeyama and co-workers proposed a fascinating design strategy for TADF materials based on a polycyclic B/N framework with the multiple resonance (MR) effect.[16] On one hand, this heteroaromatic skeleton provides adequate protection for boron atoms; on the other hand, the opposite resonance effect of boron and nitrogen atoms realizes the staggered separation of the HOMO and LUMO, which endows the resulting materials with TADF characteristics. Benefiting from the rigid conjugated framework and short-range intramolecular charge transfer (ICT) characteristics, these materials commonly exhibit emission spectra with narrow full-width at half-maximum (FWHM), high photoluminescence quantum yields (PLQYs) and the maximum external quantum efficiency (EQE_{max}) of over 20% in OLEDs.

In the light of their unique electronic structure, boron-containing derivatives have aroused wide attention and interest of scientists. By reasonably adjusting the structure, number, and linking fashion of donor and acceptor groups, OLEDs prepared with organic boron-containing functional molecules as the active layers have basically realized the full-visible emission from the blue to red region. We mainly divide the reported boron compounds into three parts, including triaryl/diarylboron-based TADF emitters, boron/oxygen (B/O)-based TADF emitters and boron/nitrogen (B/N)-based TADF emitters. In this paper, the recent research progress and prospect of organoboron-based TADF materials are reviewed systematically with emphasis on the molecular design, photophysical properties and properties of the corresponding OLEDs.

2. Highly efficient TADF emitters based on three-coordinate organoboron compounds

2.1 Triaryl/diarylboron-based TADF emitters

In 2000, Shirota and coworkers reported the first D–A type three-coordinate organoboron compounds, **1** and **2**, using diarylboron as the acceptor. In tetrahydrofuran (THF) solution, the emission peaks of **1** and **2** were at 515 nm and 537 nm, respectively. The OLEDs using **1** and **2** as emitters realized blue-green and green emission, respectively, but with a low EQE of only 0.8% and 1.0%. Thermally activated delayed fluorescence (TADF) materials have become the rising star of OLEDs by furnishing electroluminescence (EL) performance comparable with phosphorescent materials, which was initially reported by Adachi *et al.* in 2011.[17] Since then, many highly efficient triarylboron-based TADF molecules have been synthesized and their device performances are also significantly improved.

In 2015, Kaji and coworkers successfully prepared TADF emitters **3–5** applying the trimesitylboron (Mes_3B) unit as a weak acceptor, and phenoxazine (PXZ), bis(diphenylamino)-carbazole (2DAC), and diphenylaminocarbazole (DAC) as respective donors. They displayed sky-blue to green emission, high PLQYs of 87–100% in host matrices, and small ΔE_{ST} values of 0.058–0.071 eV, respectively. OLEDs using these emitters as dopants also exhibited EQE_{max} of 14.0–22.8%, respectively.[18] Later, they further reported triarylboron-based TADF emitter **6** by deliberate modulation of the RISC process. **6** possessed a relatively small ΔE_{ST} of 0.01 eV and large k_{RISC} of $1.947 \times 10^6\ s^{-1}$. The solution-processed OLED with **6** as the emitter achieved an EQE_{max} of 13.9% with an EL peak at 510 nm and CIE coordinates of (0.23, 0.54). The EQE remained at 11.7% at a luminance of 1000 cd m^{-2} with a slight efficiency roll-off of 16%.[19]

Lee and coworkers reported a synthetic approach to highly efficient D–A type TADF compounds PXZoB (**7**), DPAoB (**8**) and CzoB (**9**), wherein the acceptor was based on triarylboron and the donor was phenoxazine, diphenylamine, or carbazole. Combined with the *ortho* D–A connectivity, the bulky nature of the triarylboron endowed the D–A dyads with inherent steric "locking" for a highly twisted arrangement, leading to a small ΔE_{ST} and thus exhibiting very efficient TADF with microsecond-range lifetimes. In particular, the pure blue OLEDs based on **9** with a carbazole donor showed a high EQE_{max} of 22.6% with CIE color coordinates of (0.139, 0.150), well illustrating the validity of the proposed approach. Upon optical optimization, the EQE_{max} was further improved to 24.1%.[20] In 2017, Lu and coworkers also reported two *ortho*-D–A arranged blue TADF compounds **10** and **11**. The significant intramolecular D–A interactions induced a combined charge transfer pathway and thus achieved small ΔE_{ST} and high efficiencies. The blue non-doped OLEDs based on **10** prepared from the solution process achieved the EL emission peaking at 463 nm with an EQE_{max} of 19.1% and CIE coordinates of (0.15, 0.17).[21] Next, Lee *et al.* further developed a series of *ortho*-carbazole-appended triarylboron compounds by introducing *tert*-Bu, Me, and OMe to the carbazole donor and/or to the dimesitylphenylboron ($PhBMes_2$) acceptor. Depending on the various substituents on the donor and/or acceptor moieties, the emission color was finely tuned over the entire blue region from sky blue to ultradeep blue. Retention of a twisted D–A structure enabled by the *ortho* connectivity and bulky triarylboron led to small ΔE_{ST}. Among these, OLEDs using **12** as the emitter showed a high EQE of 32.8% with CIE coordinates of (0.135, 0.266). This high device efficiency was caused by a synergistic effect between the high PLQY (93%) and the high horizontal transition dipole ratio of 0.76. Deep blue OLEDs using **13** as the emitter showed an EQE_{max} of 14.9% with CIE coordinates of (0.151, 0.058).[22]

Lu and coworkers synthesized three D–A–D borylated compounds with functional acridan derivatives as donors and dimesitylborane as the acceptor in 2018. A small ΔE_{ST} and fast intramolecular charge transfer were caused by this crowded structure, which enabled adjacent electron donor and acceptor to form a nearly orthogonal configuration. As the ability of donors increased, the emission spectrum shifted from green to yellow region. The green device based on **14** achieved an EQE_{max} of 19.3% with CIE coordinates of (0.250, 0.527) and dropped to 18.2% at luminance levels of 1000 cd m^{-2}.[23]

In 2019, two TADF emitters **15** and **16** by introducing the cyano group into triarylboron/phenoxazine hybrids were prepared by Yang *et al.*; **15** and **16** acquired PLQYs of 67% and 75%, ΔE_{ST} of 0.144 eV and 0.077 eV, respectively. The OLEDs based on **15** and **16** achieved the EQE_{max} of 9.7% and 11.4%,

respectively, with EQEs up to 8.9% and 10.2% at 2000 cd m^{-2}. The small device efficiency roll-offs of **15** and **16** were owing to the short delayed fluorescence lifetimes of 1.6 μs and 1.4 μs, respectively.[24]

In the same year, a series of D–A–A TADF compounds **17** and **18** were obtained by Wang *et al.*, in which $(Mes)_2B$ was combined with triazine and sulfonyl units to construct tandem acceptors. These compounds possessed tiny ΔE_{ST} values contributed by the largely expanded LUMO distributions caused by the conjugation between the boron empty p-orbital and the p*-orbital of the other parts of the tandem acceptors. OLEDs based on **18** showed an EQE_{max} of 24.8% and efficiency roll-off only of 5.6% at a practical luminance of 1000 cd m^{-2}.[25]

In 2020, Chi *et al.* designed methoxy-substituted carbazoles, and the corresponding directly N-borylated emitters were prepared with the aim of improving the TADF characteristics of the carbazole-based $(Mes)_2B$ emitters. Emitters **19** and **20** showed significantly delayed fluorescence, confirming the potential of methoxy substituents in improving TADF characteristics to harness the electron-donating strength and special orthogonality. Doped devices using **19** and **20** as emitters exhibited EQE_{max} of 12.5% and 13.3%, respectively.[26]

A series of *ortho*-carbazole-appended triarylboron compounds, in which perfluoroalkyl (CF_3 and C_3F_7) or perfluoroaryl (4-$CF_3C_6F_4$) groups were attached as secondary acceptors, were prepared and characterized by Lee *et al.* in 2020. In toluene, these compounds revealed emission spectra of light greenish to yellow with high PLQYs up to 100%. The optimized OLEDs based on CF_3-substituted emitter **21** realized a high EQE of 29.9% and a low turn-on voltage of 2.35 V.[27]

Yang *et al.* constructed TADF materials **22** and **23** with the centrosymmetric 3D-A structures by connecting 9,9-diphenyl-9, 10-dihydroacridine-9 (DPAc) and 10*H*-spiro[acridine-9,9-fluorene] (SpiroAc) with triarylboron groups in 2021. These molecules possessed large dihedral angles between the triarylboron unit and the acridine plane. Because of their large volume and rigid structure, **22** and **23** showed PLQYs of 71.6% and 84.3%, respectively. Solution-processed OLEDs using **22** and **23** as emitters realized EQE_{max} of 12.8% and 17.3% with EL peaks of 472 nm and 490 nm, respectively.[28]

In 2021, by combining a weak spiro-donor and a weak spiro-acceptor through a sterically bulky p-spacer, linear D–π–A type TADF molecules with higher molecular rigidity and non-conjugated spiral fragments at both ends of the molecule were constructed by Wang *et al.* Two deep-blue emitters **24** and **25** were achieved for resolving the lack of highly efficient deep-blue OLEDs matching the display requirements. The weak D and A groups endowed the compounds with deep-blue emission and the helical structure suppressed the concentration quenching simultaneously. These emitters showed high PLQYs (>90%) in toluene. Both doped and non-doped deep-blue OLEDs based on **24** achieved an EQE of over 22% and CIE_y coordinates less than 0.1.[29]

In 2021, Lee and coworkers reported a set of D–A-type blue TADF compounds comprising triply bridged triarylboryl acceptors, the so-called B-heterotriangulenes. Compound **26** exhibited a fast RISC ($k_{RISC} \approx 10^6$ s^{-1}) with short delayed fluorescence ($\tau_d \approx 2$ μs), which was found to be promoted by the strong spin–orbit coupling between the local triplet excited state (^3LE, T_2) and the singlet (S_1) state. Devices based on **26** achieved an EQE_{max} of 28.2% and maintained an EQE of 21.2% at 1000 cd m^{-2}.[30]

In 2022, two TADF emitters with a D_3–A structure, **27** and **28**, by the combination of acridine/phenoxazine donors and triarylboron acceptors were obtained by Liu *et al.* Because of the high steric hindrance and strong intramolecular charge transfer state between the D/A groups, these emitters exhibited well-separated frontier molecular orbitals distributions and obvious TADF characteristics. The high-rigidity "star-shaped" configuration of **27** and **28** endowed both emitters with high PLQYs of up to 94% and 89%, and high ratios of horizontal dipole orientation of 86% and 80%, respectively. Doped OLEDs based on **27** and **28** realized an EQE_{max} of 38.8% and 29.4%, respectively.[31]

Triarylboron or diarylboron moieties are the simplest forms of boron acceptors that are generally used in the material design of D–A TADF emitters. The intrinsically reactive boron center is generally embraced by sterically bulky aryl groups to provide enough protection and chemical stability under ambient conditions. Three-coordinate organoboron acceptors are modified with various donors in diversified configurations to achieve small ΔE_{ST} and induce delayed fluorescence. This approach is also advantageous for tuning emission wavelength, PLQY in the solid state, and EQE in OLEDs. In this part, we summarize representative TADF emitters using three-coordinate boron derivatives as acceptors including synthetic strategies, photophysical properties and device performance. Blue to green TADF emitters have been illustrated based on a molecular platform employing three-coordinate boron-containing acceptors, and a high EQE_{max} over 30% in blue and green OLEDs has been realized. However, they suffer from a relatively broad emission spectrum because of the CT nature of S_1. Fig. 1 shows the chemical structures of various three-coordinate boron derivatives and the photophysical properties, and device performances for TADF materials discussed above are summarized in Table 1.

2.2 Boron/oxygen (B/O)-based TADF emitters

When the boron acceptor structure is modified by oxygen atoms, the acceptor strength will be weakened by the nonbonding electrons of oxygen. These boron/oxygen-based acceptors are suitable for the construction of blue TADF OLEDs. One type is a partially bridged B/O acceptor (10*H*-phenoxyaborin) by inserting an oxygen atom into the *para* position of the boron in the acceptor. Another type is the full bridged B/O acceptor (DBNA) consists of two oxygen atoms and one boron atom embedding in three benzene rings.

2.2.1 10*H*-Phenoxaborin-based TADF emitters. In 2015, Adachi *et al.* reported highly efficient blue TADF molecules, **29–31**. 10*H*-Phenoxaborin, as a new acceptor composed of a boron atom and an oxygen atom, was embedded in the aromatic backbone. Boron atoms were connected with the larger 2,4,6-triisopropyl phenyl (TIPP) groups to avoid the influence of oxygen and water. The distorted structure of the donor and the acceptor could effectively separate the HOMO and the LUMO;

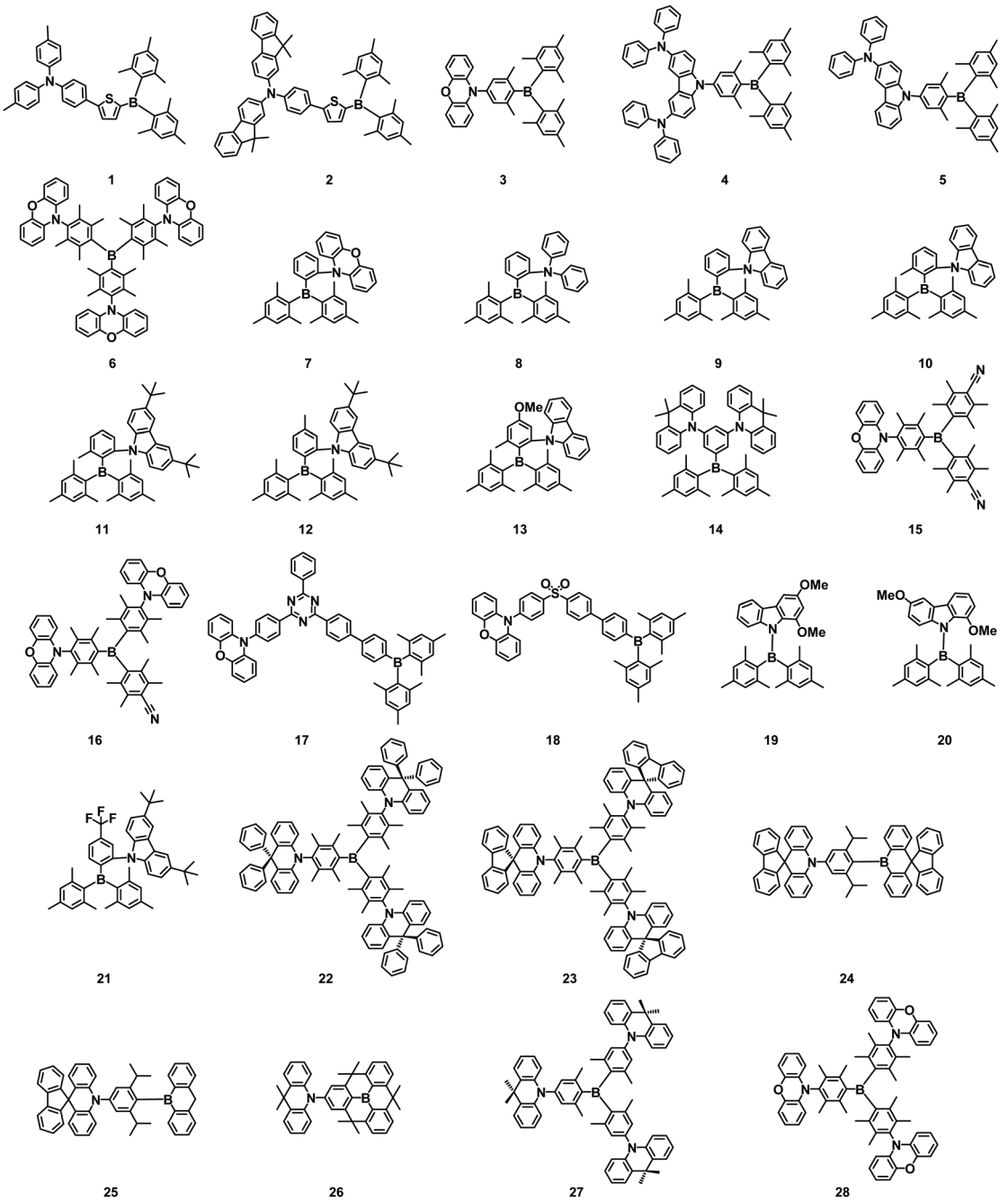

Fig. 1 Molecular structures of the TADF materials containing triaryl/diarylboron units.

thus, these emitters all possessed small ΔE_{ST}. The devices based on **30** and **31** exhibited the same CIE coordinates of (0.14, 0.16) and an EQE_{max} of 19.0% and 20.1%, respectively.[32]

Oi *et al.* designed and synthesized a series of TADF compounds using the 10*H*-phenoxaboryl group as the electron acceptor, and carbazole/9,9-dimethylacridine/phenoxazine as the electron donor. Among these, compounds **32** and **33** exhibited high PLQYs of 98% and 99%, and obvious TADF properties because the HOMO and the LUMO were well separated. The devices using **32** and **33** as emitters realized light blue and green emission, with an EQE_{max} of 15.1% and 22.1%, respectively.[33]

A new family of TADF molecules (**34–37**) with a dibenzoheteraborin unit as the acceptor were developed by Yasuda *et al.* in 2018. By introducing heteroatoms S and N into the 10*H*-phenoxyaboryl group to obtain dibenzoaborins, all the resulting emitters exhibited PLQY of nearly 100% and narrowband emission. According to the TDDFT calculation, the large spatial repulsive force between the hydrogen atoms around the D and A units limited the structural deformation between the ground and excited states and reduced the recombination energy during the emission process, resulting in narrowband emission in the TADF molecules. The up-conversion process was greatly accelerated owing to the

Table 1 Summary of the performances of TADF emitters containing triaryl/diarylboron units

Compound	PLQY[a] [%]	λ_{PL}[b] [nm]	λ_{EL}[c] [nm]	ΔE_{ST}[d] [eV]	EQE_{max}[e] [%]	CIE[f] [x, y]	Ref.
3	92	509	502	0.071	22.8	0.22, 0.55	18
4	100	495	492	0.058	21.6	0.18, 0.43	18
5	87	477	488	0.062	14.0	0.17, 0.30	18
6	65	509	510	0.01	13.9	0.23, 0.54	19
7	49	585	—	0.01	16.3	0.460, 0.505	20
8	80	498	—	0.20	21.4	0.172, 0.488	20
9	84	463	—	0.15	22.6	0.139, 0.150	20
10	61	465	463	0.06	8.0	0.15, 0.17	21
11	94	476	474	0.05	19.1	0.15, 0.26	21
12	93	478	479	0.092	32.8	0.135, 0.266	22
13	63	445	451	0.14	17.3	0.150, 0.086	22
14	46.8	505	507	0.03	19.3	0.250, 0.527	23
15	67	533	533	0.144	9.7	—	24
16	75	517	530	0.077	11.4	—	24
17	65	546	557	0.037	18.6	0.43, 0.54	25
18	84	533	535	0.013	24.8	0.37, 0.55	25
19	57	501	468	0.096	12.5	0.18, 0.24	26
20	100	452	467	0.149	13.3	0.18, 0.19	26
21	97	513	521	0.02	29.9	0.330, 0.598	27
22	71.6	474	472	0.12	12.8	0.15, 0.20	28
23	84.3	484	490	0.07	17.3	0.17, 0.40	28
24	95	453	444	0.0005	25.4	0.151, 0.058	29
25	94	448	437	0.0006	16.2	0.166, 0.066	29
26	90	462	478	0	28.2	0.136, 0.246	30
27	94	495	508	0.03	38.8	0.22, 0.52	31
28	89	553	560	0.03	29.4	0.45, 0.53	31

[a] Photoluminescence quantum yield. [b] PL emission maximum. [c] EL emission maximum. [d] Singlet–triplet energy gap. [e] Maximum external EL quantum efficiency. [f] Maximum external quantum efficiency.

heavy atomic effect of the S atom, improving the RISC rate of over 10^6 s^{-1}. Both doped and nondoped TADF OLEDs achieved a high EQE of over 20% and negligible efficiency roll-off at actual high luminance.[34]

Kwon and Lee *et al.* prepared PXB-DI (**38**) and PXB-mIC (**39**) containing oxygen-bridged, symmetric and rigid boron acceptor moieties in 2019. **38** and **39** exhibited deep-blue emission and a small singlet–triplet energy gap of 0.06 eV and 0.11 eV, respectively, in toluene. In addition, they also reported a new high triplet energy and hole transport-type host material, 5-(5-(2,4,6-triiso-propylphenyl)pyridin-2-yl)-5*H*-benzo[*d*]benzo[4,5]imidazo[1,2-*a*]imidazole (PPBI). A device with **39** in the PPBI host exhibited the EQE_{max} of 12.5% with the CIE coordinates of (0.15, 0.08). The doped device based on **38** using 2,8-bis(diphenylphosphine oxide)dibenzofuran (DBFPO) as the host achieved an EQE_{max} of 37.4%, and maintained EQE over 30% at 1000 cd m^{-2} with a small efficiency roll-off.[35]

As a continuation of the previous article, Yasuda *et al.* further also developed a series of blue TADF emitters (**40–43**) by incorporating phenazasiline, phenazagermine, and tetramethylcarbazole as weak D units and phenothiaborin as a weak A unit. The emitters all had narrow bands and allowed systematic modulation of TADF properties by changing the electron strength and rigidity of the donor. In particular, phenazasiline and phenazagermine-based emitters **40** and **42** exhibited blue emissions (464–483 nm), high PLQYs (~100%), extremely fast spin-converting reverse intersystem crossing rates ($>10^7$ s^{-1}), and suppressed concentration quenching. The doped and non-doped OLEDs based on **40** and **42** demonstrated an EQE_{max} of 27.6% and 20.9% with CIE coordinates of (0.14, 0.26) and (0.14, 0.20), respectively, and suppressed efficiency roll-offs at practically high luminance.[36] Later, they also reported excellent blue TADF emitters featuring π-extended ladder-roxaborin and thiaborin acceptors. Steady-state and time-resolved photophysical measurements revealed the advantages of the ladder-oxaborin emitter, including a tiny ΔE_{ST} of 10 meV, an ideal PLQY of 100%, and an ultrashort TADF lifetime of 780 ns. **44** and **45** achieved an EQE_{max} of up to 20.1% and 25.9% with the EL emission at 473 nm and 484 nm, respectively. As the luminance increased to 100 and 1000 cd m^{-2}, the EQE of **44** was still maintained at 19.9% and 17.6%, respectively, corresponding to a 1% and 12% roll-off.[37]

On account of the good electron-deficient ability of the triarylboron acceptor, the boron-based acceptor structure has been modified in various ways. Introduction of oxygen atoms into the boron-based acceptor structure is a promising way to construct an effective acceptor of 10*H*-phenoxaborin with the closed ring system inserted by the boron atom. By incorporating boron-based heteroaromatics into the D–A structure, many 10*H*-phenoxaborin-based compounds have been demonstrated to be effective TADF materials in OLEDs. They mostly exhibit emission in the blue region because of the relatively weak acceptor strength of 10*H*-phenoxaborin. They also can be applied in combination with other electron-donating heteroatoms, such as oxygen (E = O), nitrogen (N), sulfur (S), and selenium (Se) and offer high PLQY and high RISC rates. However, the device lifetimes of this class have not been covered, and broad spectra issues should also be resolved. The chemical structures of 10*H*-phenoxaborin-based derivatives are shown in Fig. 2, and the photophysical performances and device performances are summarized in Table 2.

2.2.2 DBNA-based TADF emitters. A one-step borylation of 1,3-diaryloxybenzenes, yielding novel boron-containing polycyclic aromatic compounds **46–49**, was performed by Hatakeyama *et al.* in 2015. These compounds possessed high singlet–triplet excitation energies as a result of localized frontier molecular orbitals induced by boron and oxygen, high PLQYs of 57–92%, small ΔE_{ST} of 0.06–0.31 eV and blue emission wavelength ranging from 418 nm to 477 nm. Using **47** and **48** as host materials, PHOLEDs with higher EQEs (20.1% and 20.6%) and significantly longer lifetimes (1000 and 383 h) than those containing CBP were obtained.[38]

Wang and coworkers reported three isomeric boron-containing sky-blue TADF emitters **50–52**, which were constructed by incorporating an electron-donor acridine (AC) moiety into *meta*-, *para*-, or *meta*′-positions of an electron-accepting boron-embedded rigid framework in 2019. The experimental results showed that the *para*-substituted compound **51** exhibited higher decomposition temperature, higher PLQY of 96%, smaller ΔE_{ST} of 0.009 eV, shorter delayed fluorescence lifetime as well as a fast RISC rate of over 10^6 s^{-1}, compared to the *meta*-isomers **50** and **52**. Bright OLEDs with EQEs up to 20.5% and 14.1% were achieved by employing **51** as doped and non-doped emitters in sky-blue OLEDs, respectively.[39]

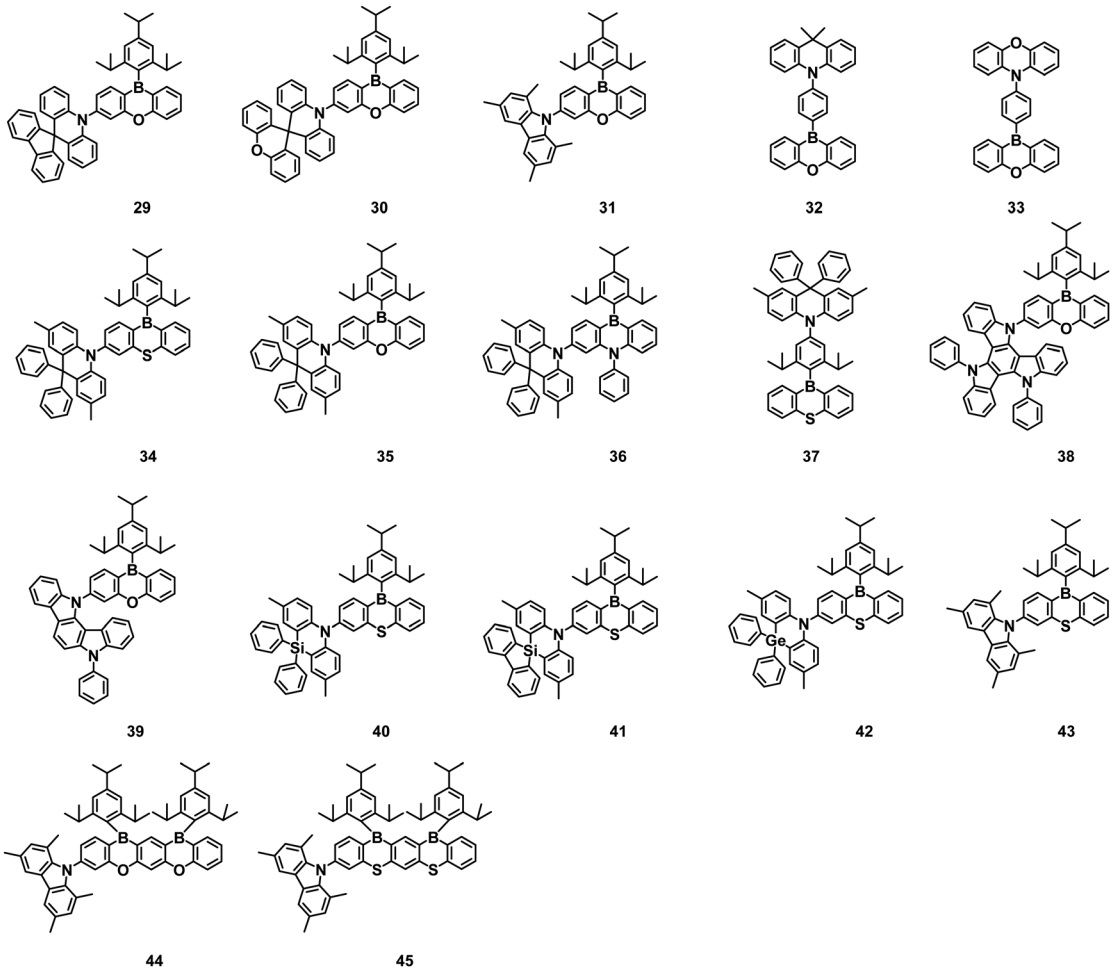

Fig. 2 Molecular structures of the TADF materials containing 10*H*-phenoxaborin units.

In 2019, Kwon *et al.* prepared two highly efficient deep-blue TADF emitters, **53** and **54**, containing oxygen-bridged, symmetric and rigid boron acceptor moieties. The 20 wt%-doped films of **53** and **54** in the DBFPO host showed a high dipole moment and high PLQYs close to 100%. The fabricated **53**-based devices using PPBI and DBFPO as hosts exhibited high EQE of 32.23 ± 0.24% and 38.15 ± 0.42%, with CIE coordinates of (0.14, 0.15) and (0.15, 0.28), respectively. The **54**-based devices using PPBI as a host realized an EQE_{max} of 21.50 ± 0.22% with CIE coordinates of (0.15, 0.06) and FWHM of 48 nm.[40] To satisfy both high efficiency and long lifetime, the Kwon group further designed and synthesized an efficient and stable blue TADF emitter **55**, which exhibited a short-delayed exciton lifetime of 1.25 μs, high PLQY of 95.3%, a small ΔE_{ST} of 0.03 eV, high k_{RISC} of 6.21×10^6 s^{-1} and good electrochemical stability. At the initial luminance of 1000 cd m^{-2}, the fabricated OLEDs displayed a high EQE of 28.1% and a long device lifetime of 329 h. The optimized OLEDs with mixed host exhibited an EQE_{max} of 26.4% and a two-folded longer lifetime of 540 h than the single host device.[41]

Choi *et al.* reported three TADF emitters **56–58** utilizing carbazole derivatives as donors and DBNA as the acceptor in 2020. Compared with the solution state, the PL intensity of these emitters was enhanced by a factor of 11–25 in the aggregated state, confirming the AIE behavior. Non-doped solution-processed OLEDs based on **56–58** exhibited EQE_{max} and CIE coordinates of 9.90% and (0.17, 0.07), 6.13% and (0.15, 0.08), and 6.04% and (0.18, 0.40), respectively.[42]

TADF emitters, **59** and **60**, connecting boron acceptor with the spiro-type spiro-biacridine (SAB) and spiro-acridine fluorene (SAF), were developed in 2020 by Kim *et al.* Because of the deep HOMO energy levels of the donors, they exhibited blue and deep-blue emissions. Benefiting from the rigid donor and acceptor, **59** and **60** showed relatively narrow emission spectra with FWHM of less than 65 nm. A high horizontal emitting dipole ratio of over 80% came from the long molecular structure along the transition dipole moment direction. The OLEDs using **59** and **60** as emitters achieved EQE_{max} of 25.7% and 28.2% and CIE coordinates of (0.144, 0.212) and (0.142, 0.090), respectively.[43]

Kwon group further reported two deep-blue TADF materials, **61** and **62**, by introducing heteroatomic sulfur and oxygen into the heavy rigid donor. As compared with **55** which possessed a similar skeleton, both emitters showed deep-blue emission below 450 nm owing to the enhancement of the optical band gap over 2.8 eV through deeper HOMO level of heteroatom-based donors. The OLEDs based on **61** and **62** demonstrated

Table 2 Summary of the performances of TADF emitters containing 10*H*-phenoxaborin units

Compound	PLQY[a] [%]	λ_{PL}[b] [nm]	λ_{EL}[c] [nm]	ΔE_{ST}[d] [eV]	EQE_{max}[e] [%]	CIE[f] [x, y]	Ref.
29	76	456	—	0.12	19.0	—	32
30	56	451	450	0.06	20.1	0.14, 0.16	32
31	86	443	—	0.12	13.3	0.14, 0.16	32
32	98	440	466	0.013	15.1	—	33
33	99	482	503	0.028	22.1	—	33
34	96	493	503	0.023	25.3	0.20, 0.51	34
35	100	477	489	0.024	24.9	0.16, 0.38	34
36	50	449	475	0.050	16.0	0.14, 0.23	34
37	91	487	500	0.030	16.4	0.19, 0.45	34
38	97	458	—	0.09	37.4	0.16, 0.34	35
39	63	438	—	0.19	12.5	0.15, 0.08	35
40	100	479	478	0.08	27.6	0.14, 0.26	36
41	100	483	484	0.06	23.9	0.14, 0.32	36
42	92	468	476	0.11	15.7	0.14, 0.22	36
43	92	476	478	0.11	21.6	0.14, 0.26	36
44	100	476	473	0.01	20.1	0.13, 0.20	37
45	93	483	484	0.17	25.9	0.14, 033	37

[a] Photoluminescence quantum yield. [b] PL emission maximum. [c] EL emission maximum. [d] Singlet–triplet energy gap. [e] Maximum external EL quantum efficiency. [f] Maximum external quantum efficiency.

the EQE_{max} of 33.2% and 32.8%, respectively. Since they both showed deep blue emissions and high efficiencies, HF-OLEDs were fabricated using ν-DABNA as a fluorescence dopant. **62** as a TADF-sensitized host in HF-OLEDs revealed an outstanding EQE of 38.8% along with narrow FWHM of 19 nm in the bottom emission pure blue OLEDs.[44]

In 2021, Choi *et al.* developed three solution-processable A–π-2D-type deep-blue emitters **63–65** by connecting two carbazole analogs as donors and a boron-fused unit as an electron acceptor to the benzene core. The luminescence mechanism of the three emitters changed from fluorescence to TADF as the donor unit was changed from carbazole to indenocarbazole, that is, only **64** and **65** exhibited TADF characteristics. Non-doped solution-processed OLEDs based on **65** showed an EQE_{max} of 10.11% and CIE coordinates of (0.16, 0.08).[45]

Yang *et al.* reported two twisted D–A type TADF materials, **66** and **67**, to solve the concentration quenching effects and serious efficiency roll-off of blue TADF materials with high horizontal dipole orientation. Significantly, **66** exhibited excellent TADF properties with a short delayed fluorescence lifetime of only 684 ns and narrow FWHM of 44 nm in the solution state, accompanied by the high PLQYs of over 80% at high doping concentrations, manifesting the alleviated exciton quenching effects. OLEDs based on **66** achieved an EQE_{max} of 29.3% and a maximum brightness of 27 663 cd cm^{-2}. Importantly, an EQE over 20% was realized even at the high brightness of 10 000 cd cm^{-2}, signifying a small efficiency roll-off.[46] In 2021, they further prepared three blue emitters **68–70**, by binding boronaphthalene [3,2,1-*de*] anthracene (BO) acceptor and acridine fluorene donors. The photophysical properties were further adjusted by substituting additional benzene at different locations of the donor to understand the relationship between the structural properties. **68** had a high k_{RISC} of 1.52×10^6 s^{-1} and **69** exhibited accelerated radiative decay when benzyl was attached to fluorene. The blue OLEDs based on **68–70** achieved EQE_{max} values of 23.9%, 20.3% and 19.3%, respectively. With the number of phenyl groups increased, CIE_y coordinates decreased to 0.197 for **69** and 0.188 for **70**, which provided a fine tuning of color purity.[47]

In 2021, Hong and coworkers obtained efficient deep-blue TADF emitters, **71** and **72** comprising almost perpendicularly linked rigid DBNA electron acceptors and a rigid linear trispiral acridine electron donor. The 10 wt% doped films of **71**, **72** in a bis[2-(diphenylphosphino)phenyl]ether oxide (DPEPO) host showed efficient TADF emission and PLQYs of 97% and 90%, respectively, because of the rigid and twisted structures and the appropriate singlet and triplet energy levels. The OLEDs based on **71** and **72** exhibited high EQE_{max} of 31.2% and 28.2%, with CIE_y coordinates of 0.092 and 0.061, respectively.[48]

By the confinement of rigid and planar N- and B-centered donor and acceptor in sandwich-type structures, the Li group obtained two molecules, **73** and **74**, which resulted in green TADF emission with up to unity efficiency and improved color purity from through-space charge-transfer excited states. With a relatively short delayed fluorescence lifetime of 11 μs, **73** demonstrated attractive green electroluminescence with an EQE_{max} of 34.9% and an EQE of 27.4% at 1000 cd m^{-2}.[49]

Because of the weak electron-accepting ability of boron acceptors, the TADF materials discussed above tend to show excellent performance in blue OLEDs. The red light-emitting materials remain limited. In 2021, Kwon and co-workers designed and synthesized two linear A–D–A orange-red TADF materials, **75** and **76**, containing rigid boron acceptors and dihydrophenazine donor moieties. They showed a small ΔE_{ST} of 0.05–0.06 eV, PLQYs as high as near unity, and a short delayed exciton lifetime (τ_d) of less than 2.63 μs in 5 wt% doped film. Doped TADF devices based on **75** and **76** showed EQE_{max} of 30.3% and 21.8%, and extremely low-efficiency roll-off (3.6% and 3.2%) at 1000 cd m^{-2}, with the EL emission peak at 576 nm and 595 nm, respectively. The devices of **75** and **76** also demonstrated high stability, with operating device lifetime (LT50) of 159 and 193 h at 1000 cd m^{-2}, respectively.[50]

The DBNA based on three adjacent boron and oxygen atoms shows relatively weak electron-withdrawing ability owing to the nonbonding electrons of oxygen. This polycyclic heteroaromatic framework with big rigidity also provides sufficient structural constraint, which enables the opposite resonance effect of boron and oxygen. As discussed above, the rigid and planar-type boron-based acceptor is effective at improving molecular stability, increasing PLQY and EQE of MR-TADF OLEDs. They show the potential as an acceptor to develop blue to green MR-TADF emitters with narrow FWHM. The above-described MR-TADF emitters containing oxygen-based fully bridged boron acceptors and different donor units are shown in Fig. 3. The photophysical properties and device performances are summarized in Table 3.

2.3 Boron/nitrogen (B/N)-based TADF emitters

2.3.1 Blue B/N-based TADF emitters. In 2015, Hatakeyama *et al.* proposed the design strategy of multi-resonance (MR) TADF materials (**77** and **78**). In such a molecule, triphenylboron possessing two nitrogen atoms was combined with neighboring

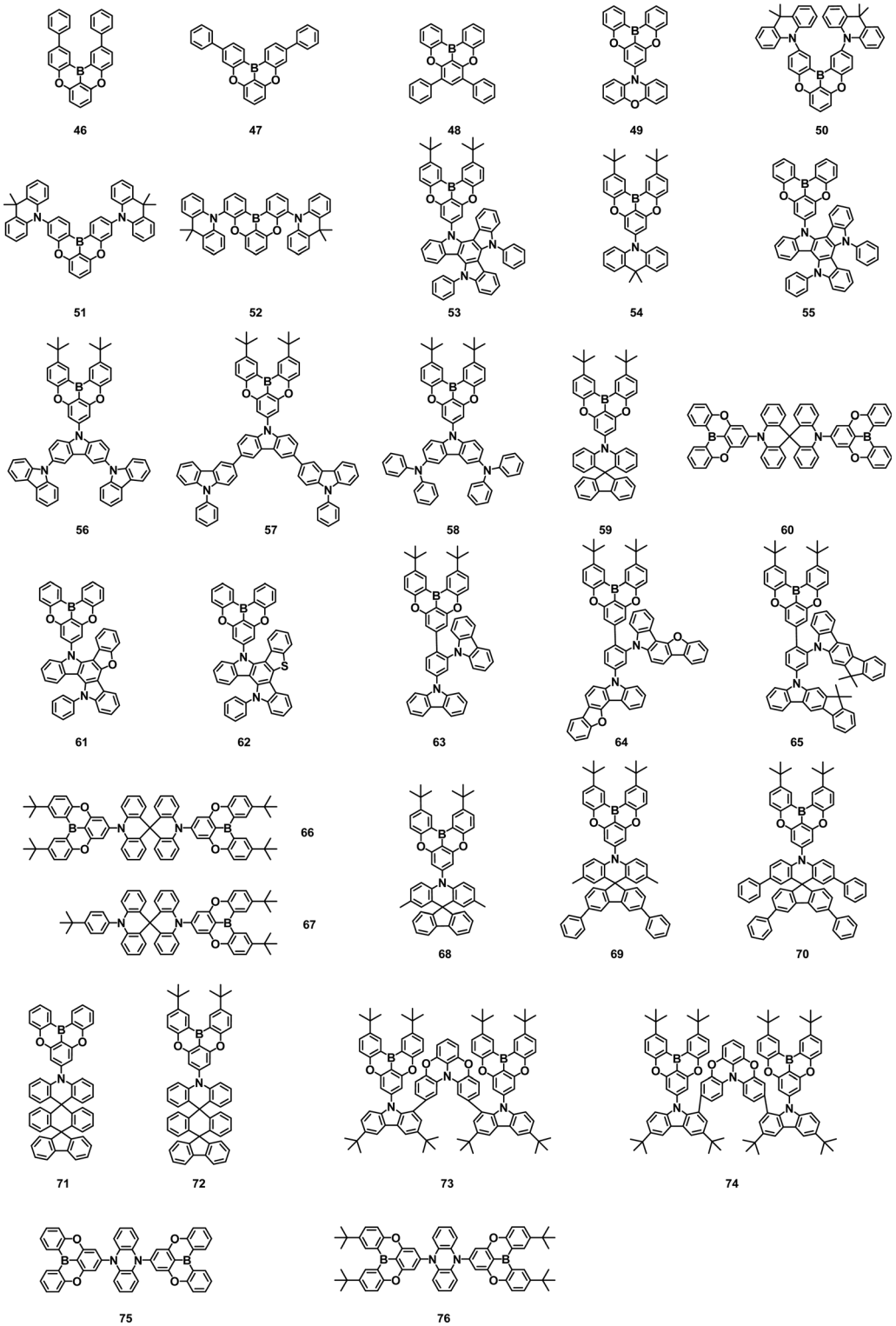

Fig. 3 Molecular structures of the TADF materials containing DBNA units.

phenyl groups to construct a rigid polycyclic aromatic framework. The nitrogen atom exhibited the opposite resonance effect of the boron atoms, which could significantly separate the HOMO and LUMO without the need to introduce donor or acceptor groups. **77** and **78** possessed small ΔE_{ST} and good color purity comparable to commercial OLEDs using filters. The device of **77** exhibited an emission peak at 459 nm, an FWHM of only 28 nm and an EQE of 13.5%. The corresponding CIE coordinates were (0.13, 0.09), which was very close to the requirements defined by the NTSC. The device employing **78**

Table 3 Summary of the performances of TADF emitters containing DBNA units

Compound	PLQY[a] [%]	λ_{PL}[b] [nm]	λ_{EL}[c] [nm]	ΔE_{ST}[d] [eV]	EQE_{max}[e] [%]	CIE[f] [x, y]	Ref.
46	65	410	—	0.21	—	—	38
47	60	410	—	0.31	—	—	38
48	57	430	—	0.14	—	—	38
49	92	492	504	0.06	13.9	—	38
50	89	492	492	0.009	17.1	0.18, 0.42	39
51	96	496	488	0.009	20.5	0.17, 0.36	39
52	87	498	492	0.031	14.1	0.18, 0.39	39
53	99	456	—	0.11	38.15	0.15, 0.28	40
54	93	458	448	0.06	25.71	0.14, 0.15	40
55	95.3	467	475	0.03	28.1	0.16, 0.39	41
56	99	433	424	0.064	9.9	0.17, 0.07	41
57	93	460	448	0.113	6.13	0.15, 0.08	41
58	90	494	492	0.072	6.04	0.18, 0.40	42
59	90	—	456	0.11	28.2	0.142, 0.090	43
60	87	—	472	0.07	25.7	0.144, 0.212	43
61	96.9	446	476	0.17	33.2	0.15, 0.24	44
62	94.8	445	476	0.29	32.8	0.15, 0.24	44
63	61.0	414	412	—	3.44	0.18, 0.10	45
64	86.4	423	416	0.26	6.78	0.17, 0.07	45
65	75.5	431	424	0.15	10.1	0.16, 0.08	45
66	87	448	475	0.01	18.3	0.13, 0.21	46
67	89	450	467	0.01	29.3	0.13, 0.15	46
68	99	477	473	0.01	23.9	0.141, 0.215	47
69	98	472	470	0.02	20.3	0.139, 0.197	47
70	80	475	471	0.20	19.3	0.143, 0.188	47
71	97	452	452	0.057	31.2	0.147, 0.092	48
72	90	446	448	0.079	28.2	0.149, 0.061	48
73	100	502	502	0.03	31.4	0.21, 0.50	49
74	86	518	508	0.11	34.9	0.23, 0.54	49
75	99.8	599	576	0.06	30.3	0.49, 0.50	50
76	85.4	610	595	0.05	21.8	0.55, 0.45	50

[a] Photoluminescence quantum yield. [b] PL emission maximum. [c] EL emission maximum. [d] Singlet–triplet energy gap. [e] Maximum external EL quantum efficiency. [f] Maximum external quantum efficiency.

exhibited pure blue emission at 467 nm with a narrow FWHM of 28 nm, CIE coordinates of (0.12, 0.13), and an IQE of ≈100%, which represented record-setting performance for blue OLEDs at that time.[16]

Based on the innovative design strategy of MR-TADF materials, scientists have devoted a lot of effort to obtaining new narrowband B/N compounds. We have summarized the representative design method, hoping to provide instructive guidance for further research of MR-TADF materials. The first method is to use DNBNA as the base skeleton to obtain the blue narrowband materials by directly introducing peripheral modification without changing the B/N core.

In 2018, Huang and coworkers synthesized **79** by introducing a peripheral carbazole group in the *para* position of the B-substituted phenyl-ring. The introduction of a carbazole unit could significantly boost the resonance effect without compromising the color fidelity. In toluene, **79** had an FWHM of 26 nm and a PLQY of 97.48%. The corresponding OLEDs exhibited excellent performance with an EL emission at 474 nm, an EQE_{max} of 32.1% and CIE coordinates of (0.12, 0.19).[51]

Subsequently, Lee and coworkers reported a blue MR-TADF molecule **80**. They developed a device structure by using a TADF assistant dopant to enhance fluorescence emission of B/N type blue TADF emitters, named the TATADF device, which underwent a RISC-mediated cascade energy transfer. The combination of **80** and the TATADF device structure enabled a high EQE greater than 30%, pure blue emission color coordinates of (0.13, 0.15), a narrow FWHM of 31 nm and a lifetime improvement by more than 10 times.[52] Later, they further reported a deep blue TADF molecule **81**, which was resistant to the concentration quenching effect by introducing the di(*tert*-butylphenyl)amine group at the *para* position of the boron element. The additional tDPA donor promoted RISC, resulting in a three-times higher k_{RISC} of **81** than that of *t*-DABNA. OLEDs based on **81** reached an EQE_{max} of 27.9%, CIE coordinates of (0.13, 0.08) and FWHM of 26 nm.[53] As an extension of the previous article, the Lee group also reported a pure blue TADF molecule **82**, which possessed an additional di-*tert*-butylphenyl substituted group on *t*-DABNA to reduce quenching of the intermolecular interaction. The single-layer device of **82** exhibited FWHM of 22 nm and EQE of 11.4%. The device lifetime was up to LT95–208 hours at 1000 cd m^{-2} and more than 10 000 hours at 100 cd m^{-2}. The optimized tandem device of **82** achieved an EQE_{max} of 30.1%, which exhibited long LT95 of over 30 000/500 h observed at 100/1000 cd m^{-2}.[54]

In 2021, Wang's group designed and synthesized three deep blue narrowband MR TADF emitters **83–85** by using the periphery cladding strategy. The intermolecular interactions were suppressed by cladding a large steric hindrance *tert*-butyl unit at the periphery of the MR emitter, leading to a reduced emission quenching and improved PLQY. The **85**-based device with 1,3-di(9*H*-carbazol-9-yl)benzene (mCP) as host exhibited an EQE_{max} of 19.3%, CIE coordinates of (0.141, 0.076) and FWHM of 26 nm, respectively.[55]

B/N-based emitters are usually affected by strong π–π interactions due to their rigid planar structure. In 2022, Kim and coworkers developed blue MR-TADF **86** through a simple synthetic process by introducing *meta*-xylene and *meta*-phenyphenyl groups to the core to inhibit the interaction between molecules. As a result, highly efficient pure blue OLEDs with an EQE_{max} of 24.3%, CIE coordinates of (0.124, 0.140), and FWHM of 28 nm were realized. The corresponding EL emission spectra can be maintained even at a high doping concentration of over 20%.[56] In the same year, they reported another isomer **87**. Compared with **86**, emitter **87** also could effectively suppress the intermolecular interactions deriving from the π–π repulsion between the biphenyl units and the steric hindrance between *ortho*-xylyl groups. Adding biphenyl moieties to the core body created dense local triplet states in the vicinity of S_1 and T_1 energetically, letting the emitter harvest excitons efficiently. As a result, k_{RISC} of **87** (6.85×10^4 s^{-1}) was three times higher than that of **86** (1.95×10^4 s^{-1}). The OLED based on **87** showed a high EQE of 23.4%, with an FWHM of 22 nm and CIE coordinates of (0.133, 0.109). By incorporating a conventional TADF sensitizer, the related device achieved deep blue emission with CIE coordinates of (0.133, 0.109) and extremely high EQE_{max} of 30.1%.[57]

An alternative strategy to obtain blue MR-TADF emitter involves the modification of the conjugate skeleton of MR-TADF by facilely extending the aromatic rings and expanding the HOMO and LUMO distribution to increase the solubility, enhancing the efficiency and modulating emission color.

In 2020, Chen *et al.* synthesized two molecules, **88** and **89**, by replacing diphenylamine with carbazole groups and introducing *tert*-butyl groups into the MR skeleton. **88** and **89** exhibited sky-blue and bluish-green emission. It was found that the extension of π-conjugation and the introduction of electron-donating moieties at N-resonance positions to enhance the MR effect could narrow the bandgap and bathochromic-shift the emission spectra for small ΔE_{ST}, increased PLQY and good solubility. Unprecedentedly, the first solution-processed MR-TADF OLEDs showed the maximum CEs of 31.1 and 24.3 cd A^{-1}, PEs of 19.5 and 15.9 lm W^{-1} and EQE_{max} of 16.3 and 14.7% for **88** and **89**-based devices, respectively.[58]

Adachi *et al.* reported the utilization of a classic BN skeleton to construct two narrow-emission materials, **90** and **91**. The introduction of a carbazole unit in the BN skeleton could fine-tune the energy level and enhance PLQY, while good color purity and fast radiation decay were retained. It was found that the smaller E_{HOMO} difference between the TADF-assisted dopant and the terminal emitter helped to reduce hole capture in the emission layer, resulting in a lower efficiency roll-off and a longer device lifetime. Blue TADF-assisted fluorescence TAF-OLEDs based on **90** and **91** as terminal emitters were fabricated, resulting in a high EQE of up to 21.9%, high color purity, and a high brightness of 63 777 cd m^{-2} with a small efficiency roll-off (EQE of 21.2% and 19.8% at 100 and 1000 cd m^{-2}, respectively).[59]

Hatakeyama and coworkers synthesized carbazole-based DABNA analogue **92** from triarylamine by regioselective one-shot single and double borylation. The reaction proceeded selectively at the *ortho* position of the carbazolyl group, where the highest occupied molecular orbital was mainly localized owing to the difference in the electron-donating abilities of the diarylamino and carbazolyl groups. The device using **92** as the emitter showed narrowband sky-blue emission with an EQE_{max} of 21.8% and CIE coordinates of (0.11, 0.23).[60]

Yang *et al.* also developed a series of asymmetric MR-TADF emitters, **93–95**, in 2021. In toluene, they all exhibited similar blue emission in the 460 to 469 nm range with FWHM values as low as 20 to 23 nm. By the peripheral decoration design strategy, the diphenylaniline group was introduced into the basic molecule **93** to adjust the photophysical properties, which could maintain PLQY of over 90%, reduce the spectral widening and improve the RISC rate. Among the three OLEDs based on **93–95**, the EQE_{max} was 23.6, 24.0 and 27.7%, and the FWHM was reduced from 34 nm to 28 nm and 24 nm, respectively.[61] In 2022, they obtained two MR-TADF compounds **96** and **97** with gradually enlarged ring-fused structures and increased rigidity from the same precursor by lithium-free boration. The extension of the MR skeleton enhanced molecular rigidity, resulting in smaller structural relaxation energy, increased oscillator strength and improved RISC process. OLEDs based on **96** and **97** revealed emission peaks of 457/467nm, FWHM of 28/23 nm, and the EQE_{max} of 31.2/33.2%.[62]

In 2022, two blue TADF emitters **98** and **99** using acridan-containing arylamine derivatives as the starting materials of electrophilic C–H borylation reaction were prepared by Wang *et al.* These compounds had high PLQYs (94.4% and 89.7%) and narrow FWHMs (19 nm and 26 nm). The OLEDs utilizing **98** and **99** as emitters exhibited EQE_{max} of 21.6% and 22.3% and CIE coordinates of (0.135, 0.094) and (0.116, 0.186), respectively. The electrophilic borylation site of the borylation reaction could be controlled by varying the steric hindrance effect and electron-donating ability of the substrate substituent. The different HOMO distribution originated from the differences in the substrate substituent accounted for different cyclization modes for **98** and **99**.[63]

A "self-host" strategy was developed by Xu *et al.* to achieve blue MR-TADF emitter **100** by integrating host segments into the MR skeleton without involving additional charge transfer and/or vibrational components to excited states. At a doping concentration of up to 30%, **100** exhibited a blue emission peak at 472 nm, vibrator intensity ≈0.5, radiation rate of up to 2.11×10^8 s^{-1} and exponentially reduced the non-radiation rate constant. Consequently, at the same time as preserving narrowband blue emission with an FWHM of ≈28 nm at a high doping concentration of 30%, **100** revealed state-of-the-art PLQY of 99% and an EQE_{max} of 30%, respectively.[64]

The design strategy of introducing heteroatoms (O/S/Se, *etc.*) into the MR skeleton is also commonly applied to finely modulate emission colors. For example, in 2021, Yasuda *et al.* designed a new family of MR-TADF materials that could exhibit narrowband emissions ranging in color from deep blue to yellow. By introducing the electron-withdrawing imine and electron-donating amine moieties into the common boron-embedded MR skeleton (Cz-B), systematic hypsochromic and bathochromic shifts of narrowband TADF emissions could be achieved, allowing effective luminescence color tuning over a wide visible range without degrading the intrinsic high PLQY. Consequently, the corresponding narrowband deep-blue to yellow OLEDs achieved an EQE_{max} of 19.0–29.2% with desirable EL color purity. The **101**-based blue device exhibited an emission peak at 461 nm, a FWHM of 28 nm, and an EQE_{max} of 19.0%.[65]

A series of asymmetric blue MR TADF emitters **102–105** were prepared by Lee *et al.* in 2021. They had an asymmetric molecular structure with one boron, one oxygen, and one nitrogen. The aromatic units linked to the nitrogen were changed into diphenylamine, carbazole, dimethylacridine, and diphenylacridine to manage the light emission properties of the emitters. It was found that they all exhibited emission in the blue region due to the weak electron-donating oxygen atom and the emission wavelength was controlled by the aromatic unit connected to the nitrogen. The **102**-based OLEDs possessed an EQE_{max} of 16.3%, a FWHM of 32 nm, and CIE coordinates of (0.15, 0.05).[66]

Yang *et al.* also elaborately constructed three oxygen-containing blue MR materials **106–108**, which utilized the opposite MR effect of B and N/O atoms to achieve TADF characteristics. The **106**-based deep blue OLEDs achieved an EQE_{max} of 13.6%, an FWHM of 36 nm with CIE coordinates of (0.14, 0.08). Devices assisted by a sensitizer based on **107** and **108** exhibited an EQE of up to 29.6% with a relatively small efficiency roll-off.[67] They further reported a blue MR TADF material **109** with gradual peripheral modification in a boron/nitrogen (B/N) embedded polycyclic skeleton. The ternary TADF-sensitized device based on

109 realized blue emission peaking at 468 nm with an EQE_{max} of 32.0%.[68] In 2022, Shao *et al.* designed solution-processed MR dendrimers **110–111** by introducing carbazole dendrons in the periphery of the B,O,N-doped polycyclic aromatic skeleton. **110–111** could keep the narrowband emission and suppress aggregation quenching by steric carbazole dendrons. Solution-treated OLEDs based on **110** realized the EL at 488 nm with a FWHM of 39 nm and an EQE_{max} of 13.4%.[69] Wang and co-workers reported two kinds of B, Se, and N-doped polycyclic aromatic hydrocarbons (PAH) narrowband blue emitters (**112–113**). Benefiting from the heavy atom effect of Se, they exhibited a strong spin–orbit coupling and fast RISC rate ($7.5–8.8 \times 10^6$ s^{-1}), which was 2 orders of magnitude faster than conventional MR-TADF molecules. The **112**-based OLEDs showed blue emission at 481 nm, FWHM of 32 nm, and the EQE_{max} of 22.3%.[70] Subsequently, they also reported two blue emitters **114** and **115** by replacing Se with S. The device with **115** as the emitter exhibited an emission peak at 473 nm, a FWHM of 29 nm and an EQE_{max} of 22.0%.[71]

The fourth method is to introduce double or more boron atoms into the MR skeleton by borylation reactions to obtain narrowband blue emitters with even higher performance in OLEDs. In 2017, Hatakeyama and co-workers developed one-shot double, triple, and quadruple borylation reactions of triarylamines through a judicious choice of boron source and Brønsted base. With the aid of borylation reactions, a variety of BN-doped nanographenes **116–118** were synthesized in two steps starting from commercially available materials. OLEDs employing BN-doped nanographene as an emitter exhibited deep pure blue emission at 460 nm, with CIE coordinates of (0.13, 0.11), and an EQE_{max} of 18.3%.[72] In 2019, they succeeded in the synthesis of novel TADF materials with two boron and one nitrogen atom, **119–120**, *via* nucleophilic substitution and electrophilic C–H borylation. The k_{RISC} values of these B–N–B molecules (7.6×10^3 s^{-1}, 9.0×10^3 s^{-1}) were comparable to N–B–N-type DABNA-1 (11.1×10^3 s^{-1}), and the emission wavelength was slightly redshifted without broadening of the emission band. The OLEDs using **120** as the emitter exhibited sky blue emission at 480 nm with an FWHM of 33 nm and a maximum EQE of 21.4%.[73] In 2019, Hatakeyama reported a blue emitter, **121**, in which the MR core consists of five benzene rings embedded with two boron and four nitrogen atoms, and simultaneously two diphenylamine substitutions on the periphery. MR-TADF with this double *meta* B–π–B structure had a fully resonant extended π-skeleton, which can inhibit the emission redshift. The MR effects of boron and nitrogen atoms induce significant localization of the HOMO and LUMO on different atoms, minimizing their bonding/antibonding properties and vibration coupling between ground and excited states, leading to an unprecedented ultra-narrow FWHM spectrum of only 14 nm. OLEDs using **121** as the emitter reached the EQE_{max} of 34.4%, a pure blue emission at 469 nm, CIE coordinates of (0.12, 0.11) and an FWHM of 18 nm. Moreover, the device's efficiency roll-off was greatly suppressed with an efficiency of 32.8% at 100 cd m^{-2} and 26.0% at 1000 cd m^{-2}, respectively.[74] Later, the Hatakeyama group further synthesized an ultrapure blue MR-TADF material **122** based on **121** by introducing an oxygen atom. **122** showed a hypsochromic shift compared to the parent MR-TADF material, because of restricted π-conjugation by oxygen atom incorporation. The OLEDs using **122** as the emitter realized an EL emission peak at 465 nm, an FWHM of 23 nm, CIE coordinates of (0.13, 0.10) and an EQE_{max} of 29.5%. Compared with the device of **121**, the **122**-based device provided considerably lower efficiency roll-off and longer device lifetime (LT50 = 314 at 100 cd m^{-2}).[75]

In 2021, Yasuda *et al.* reported a series of **121**-based MR emitters **123–125** with exquisite combination and interplay of multiple boron, nitrogen, oxygen, and sulfur heteroatoms embedded in a fused polycyclic π-system. Because oxygen and sulfur atoms have weak electron-donating capacity, the emission color could be finely modulated while maintaining a narrow bandwidth. These emitters exhibited ultra-pure narrowband blue emission peaks at 445–463 nm, PLQYs of 64–93%, FWHM of 18–23 nm, and CIE_y coordinates of 0.04–0.08. The OLEDs using **124–125** as emitters showed the EQE_{max} of 26.9% and 26.8% with CIE coordinates of (0.14, 0.06) and (0.13, 0.08), respectively.[76] Afterwards, they demonstrated the strategic implementation of electron-accepting tricoordinate boron and electron-donating carbazole subunits into PAHs to produce a family of attractive full-color luminophores with narrowband emission. Among these, the sky-blue emitter **126** showed an EL peak at 471 nm, FWHM of 26 nm and EQE_{max} of 29.3%. With a similar design strategy, a nanographitic fused-nonacyclic p-system **127**, which was strategically embedded with multiple boron, nitrogen, and sulfur atoms, was also developed by them. Narrowband sky-blue emission with a peak at 478 nm, an FWHM of 24 nm, a PLQY of 89% and an EQE_{max} of 29.3% was obtained in **127**-based OLEDs.[77,78]

Later, Wang *et al.* found a new reaction that proceeded slowly at room temperature and accelerated at high temperature, paving the way for new, milder procedures for the preparation of B-doped PAHs with high yields and functional group tolerance. Furthermore, the potential of this B-PAH synthesis has been demonstrated by the successful and highly divergent synthesis of a series of B,N,B-doped benzo[4]helicenes **128–131**. These ADBNA derivatives showed PL emission peaks at 482–487 nm and PLQYs of 71–88% in CH_2Cl_2.[79] A "one-pot" catalyst-free borylation method was developed by Duan *et al.* in 2022, which generated deep-blue to pure green MR-TADF emitters by readily peripheral decoration and skeleton fusion of BCzBN. The device based on blue emitter **132** achieved an emission peak at 431 nm with an EQE_{max} of 13.5% and CIE coordinates of (0.16, 0.05).[80]

In 2021, Kown *et al.* developed three deep-blue MR-TADF compounds **133–135** by incorporating methyl groups and fluorine atoms in a diboron-based core. The introduction of methyl groups at *para* positions to the boron atoms and fluorine atoms at *ortho* positions to the nitrogen atoms resulted in bandgap enhancement by electron-donating and electron-withdrawing effects. All three emitters exhibit pure blue emissions with high PLQYs around ~90%, and small ΔE_{ST} ($\leq$0.07 eV) values. Among three materials, **134** and **135**-based OLEDs demonstrated CIE_y coordinates of 0.08 and 0.06, and the EQEmax of 35.8% and 33.7%, respectively.[81] Further, they reported two deep blue MR-TADF emitters, **136** and **137**, using double boron, three nitrogen and two oxygen atoms. Both materials showed deep blue emissions of ~450 nm with a high PLQY of ~90%.

These materials showed very small ΔE_{ST} less than 0.06 eV and a high rate of reverse intersystem crossing of $\sim 2.5 \times 10^5$ s^{-1}. The TADF devices based on **136** and **137** showed EQE_{max} of 30.7 and 32.5%, and CIE_y coordinates of 0.06 and 0.07, respectively, which satisfy the requirements of blue BT2020.[82]

Several triple boron-containing MR-TADF compounds with linear structures and V-shaped B–π–B structures have also been developed. In 2020, Zysman-Colman *et al.* reported a rare example of non-triangulene-based MR-TADF emitter **138**, which simultaneously possessed narrow, deep-blue emission with CIE coordinates of (0.17, 0.01). They also synthesized **139** with a similar structure as a derivative of **138**. The red-shifted and more intense absorption allowed **139** to pair with a high-performance TADF assistant dopant and achieved an EQE_{max} of 15%, FWHM of 49 nm at color coordinates of (0.15, 0.10).[83,84] In 2022, the Hatakeyama group synthesized MR-TADF molecule **140** with an expanded heterohelicene consisting of three BN_2-embedded [4]helicene subunits. Based on the MR effect of three boron and six nitrogen atoms, **140** exhibited a narrowband sky-blue emission with an FWHM of 16 nm. Solution-treated OLEDs with **140** as the emitter showed emission wavelength at 480 nm, FWHM of 27 nm and an EQE_{max} of 22.9%.[85] They also reported two V-shaped MR-TADF materials **141–142**. The inductive effect of fluorine atoms reduced the HOMO energy of **141**, leading to the blue-shifted emission peak (464 nm) compared with that of **141** (481 nm). **142** demonstrated a small FWHM of 16 nm and a high RISC rate constant (6.5×10^5 s^{-1}). OLEDs using **141–142** as emitters exhibited blue emission at 483 and 468 nm, with FWHMs of 17 and 15 nm and CIE coordinates of (0.09, 0.27) and (0.12, 0.10), respectively. At 1000 cd m^{-2}, both devices achieved high EQE of 26.2% and 26.6%, with tiny efficiency roll-off of 0.9% and 3.2%.[86]

Blue, green, and red are three fundamental colors for organic EL displays. Thus, organic blue, green, and red luminogens with superhigh color purity are of significant importance for achieving a wide color gamut in OLEDs. Organic light-emitting materials generally showed broad emission spectra and poor color purity, which remains one of the major challenges in OLEDs for many years. The pioneering discovery of blue B/N-containing MR-TADF materials has laid a reliable foundation for the development of organic light-emitting materials with narrow-band emission and provided high potential for the manufacture of OLEDs with ultrahigh color purity. In fact, blue TADF OLEDs are of high interest since they are considered as promising alternatives to commercial fluorescent blue materials. In this part, blue MR-TADF materials containing DABNA units that possess maximum EL peaks below 490 nm are summarized in Fig. 4 and Table 4.

2.3.2 Green B/N-based TADF emitters. As one of the three primary colors, green emitters play an important role in the field of display. So far, scientists have developed a number of green MR-TADF compounds using the similar design strategy described above. In 2019, bis(di(*t*-butyl)carbazolyl)phenylene was first employed by Wang *et al.* as a parent skeleton to construct B–N-containing compound **143** with a large and rigid π-conjugated core skeleton. To further red shift the emission to the green region, expansion of conjugation was carried out by introducing four C_6H_4 groups to the carbazolyl moieties, and

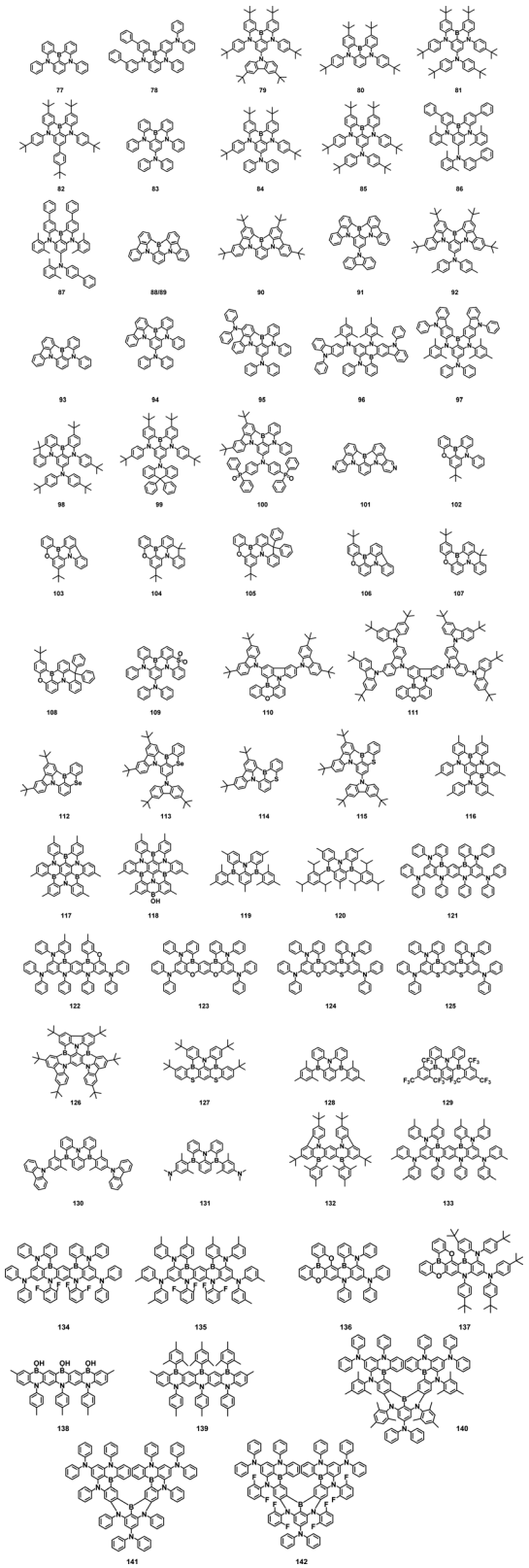

Fig. 4 Molecular structures of blue B/N-based TADF emitters containing DABNA units.

Table 4 Summary of the performances of blue B/N-based TADF emitters containing DABNA units

Compound	PLQY[a] [%]	λ_{PL}[b] [nm]	λ_{EL}[c] [nm]	ΔE_{ST}[d] [eV]	EQE_{max}[e] [%]	CIE[f] [x, y]	Ref.
77	88	460	459	0.20	13.5	0.13, 0.09	16
78	89	469	467	0.20	20.2	0.12, 0.13	16
79	97	470	474	0.14	32.1	0.12, 0.19	51
80	88	—	466	0.17	31.4	0.13, 0.15	52
81	96	446	459	0.10	27.9	0.13, 0.08	53
82	97	465	471	0.19	11.4	0.11, 0.16	54
83	60.8	449	456	0.06	14.7	0.145, 0.076	55
84	67.3	456	456	0.08	16.8	0.145, 0.076	55
85	74.7	456	460	0.10	19.3	0.141, 0.076	55
86	97	464	468	0.12	24.3	0.124, 0.140	56
87	98	462	464	0.176	23.4	0.132, 0.092	57
88	87	478	480	0.12	14.7	—	58
89	86	498	490	0.11	16.3	—	58
91	92	465	471	0.18	21.9	0.160, 0.305	59
92	85	478	477	0.14	21.8	0.11, 0.23	60
93	98	469	475	0.11	23.6	0.14, 0.30	61
94	92	460	469	0.12	24.0	0.13, 0.16	61
95	94	468	472	0.13	27.7	0.12, 0.18	61
96	91	454	457	0.20	31.2	0.14, 0.08	62
97	93	464	467	0.16	33.2	0.13, 0.11	62
98	94.4	454	460	0.17	21.6	0.135, 0.094	63
99	89.7	468	472	0.15	22.3	0.116, 0.186	63
100	99	466	472	—	30.8	0.14, 0.22	64
101	83	460	461	0.12	19.0	0.13, 0.13	65
102	86	433	443	0.18	16.3	0.15, 0.05	66
103	94	441	481	0.15	13.4	0.13, 0.22	66
104	91	461	475	0.11	16.2	0.12, 0.21	66
105	94	463	473	0.06	17.0	0.12, 0.20	66
106	96	443	454	0.21	13.6	0.14, 0.08	67
107	99	462	472	0.23	20.4	0.13, 0.19	67
108	98	462	468	0.19	23.0	0.13, 0.14	67
109	98	468	476	0.17	32.0	0.15, 0.24	68
110	94	476	488	0.14	13.4	0.13, 0.44	69
111	98	472	487	0.10	14.9	0.15, 0.45	69
112	87	479	490	0.15	20.3	0.13, 0.45	70
113	93	472	481	0.14	22.3	0.11, 0.25	70
114	82	476	482	0.13	18.9	0.11, 0.28	71
115	88	463	473	0.12	22.0	0.11, 0.17	71
116	53	461	460	0.19	18.3	0.13, 0.11	72
117	33	442	—	0.15	—	—	72
118	37	449	—	0.15	—	—	72
119	89	484	481	0.18	16.2	0.10, 0.27	73
120	88	482	480	0.18	21.4	0.11, 0.29	73
121	90	467	469	0.017	34.4	0.12,0.11	74
122	—	464	465	0.029	29.5	0.13, 0.10	75
123	76	441	445	0.15	16.6	0.15, 0.04	76
124	94	453	455	0.159	33.1	0.14, 0.06	76
125	93	460	463	0.144	32.2	0.13, 0.08	76
126	93	466	469	0.15	29.3	0.12, 0.18	77
127	89	478	478	0.14	21.0	0.11, 0.22	78
128	71	482	—	0.18	—	—	79
129	85	487	—	0.19	—	—	79
130	81	486	—	0.17	—	—	79
131	18	481	—	0.13	—	—	79
132	68	431	431	0.31	13.5	0.16, 0.05	80
133	90.5	464	471	0.07	36.2	0.12, 0.12	81
134	90.2	457	464	0.05	35.8	0.13, 0.08	81
135	88.9	455	461	0.07	33.7	0.13, 0.06	81
136	88.1	445	455	0.05	30.7	0.14, 0.06	82
137	90.3	451	460	0.06	32.5	0.14, 0.07	82
138	50	390	—	0.31	—	—	83
139	63	442	443	0.28	14.6	0.15, 0.10	84
140	80	484	480	0.004	22.9	0.09, 0.21	85
141	90	481	483	0.006	26.2	0.09, 0.27	86
142	81	464	468	0.005	26.6	0.12, 0.10	86

[a] Photoluminescence quantum yield. [b] PL emission maximum. [c] EL emission maximum. [d] Singlet–triplet energy gap. [e] Maximum external EL quantum efficiency. [f] Maximum external quantum efficiency.

144 was thus successfully obtained. Based on the combination of TCTA:PIM-TRZ exciplex cohost and **144** dopant, a high-performance green fluorescent OLED with an EQE_{max} of 25.5% and FWHM of 33 nm was achieved. More importantly, the CIE coordinates of (0.20, 0.65) were quite close to the NTSC green-light standard (CIE: (0.21, 0.71)).[87] Next, they proposed a molecular design strategy based on frontier molecular orbital engineering, which could integrate the advantages of a twisted D–A structure and an MR skeleton. By introducing an auxiliary electron-donor moiety into a HOMO-localized *meta*-carbon position relative to the B-substituted phenyl ring within the 1,3-bis(carbazol-9-yl)benzene-based MR framework, **145** was obtained with emission maximum beyond 520 nm and narrow FWHM. The device based on **145** achieved an EQE_{max} of 27.0% and CIE coordinate of (0.23, 0.69).[88] Later, in order to simplify the synthesis process and enhance the reaction yield, they provided a synthetic methodology to functionalize MR skeletons and a universal building block DtCzB-Bpin was generated, which could be utilized to construct TADF materials through a simple one-step Suzuki coupling reaction. Based on this synthetic strategy, green TADF emitters **146–149** were obtained by localized attachment of 1,3,5-triazine and pyrimidine derivatives-based acceptors onto MR frameworks with 1,3-bis(3,6-di-*tert*-butylcarbazol-9-yl)benzene (DtCz) as the ligand. Among these molecules, the **147**-based device showed a CIE coordinate of (0.23, 0.68), an EQE_{max} of 30.6%, an EL peak at 520 nm and an FWHM of 41 nm.[89] Then, with a similar design method, a phenyl bridge was inserted between the donor and the MR framework to guarantee the red-shift emission and also avoid strong ICT. Four narrowband molecules by introducing donor, acceptor, and neutral units in the *para*-position of the *N*-substituted benzene ring in a brominated MR framework were gained. Among them, OLEDs of **150** realized pure green emission at 500 nm, an FWHM of 28 nm and a record-high EQE_{max} of 40.6%.[90]

In 2019, by amplifying the influence of the skeleton and the peripheral units, Duan *et al.* synthesized a series of efficient green MR-TADF materials, **151–154**. The electron-accepting groups expanded the distribution of LUMO, enhanced ICT characteristics, and thus narrowed the energy gap. The OLEDs based on **152–154** showed EL peaks at 501, 499, 493 nm, EQE_{max} of 22.0, 22.7, and 20.9%, and the FWHM of 30–40 nm, respectively.[91] In 2020, the Yasuda group also reported two green MR compounds, **155** and **156** by introducing multiple *tert*-butylcarbazole groups around the periphery. OLEDs of **155** and **156** realized EL emission peak at 515/549 nm, FWHMs of 54/48 nm and EQE_{max} of 31.8/29.3%.[77]

For MR systems, it is found that emission regulation can be achieved by introducing the electron-donating units into the carbazole of the MR skeleton. In 2021, Yasuda and co-workers used this design strategy to synthesize two MR compounds **157–158**, without compromising narrow spectral features. Because the HOMO extended to the peripheral donors, the energy gap became narrowed, resulting in a redshifted emission wavelength. The OLEDs of **157–158** revealed an EL peak at 515/571 nm, an FWHM of 30/34 nm, and an EQE_{max} of 29.2/19.6%, respectively.[65] Similarly, by manipulating the numbers

and electron-donating abilities of the peripheries, **159–161** were obtained by Yang *et al.* **161** realized the first narrowband yellow emitter with emission maxima of 562 nm, an FWHM of 30 nm and an EQE_{max} of 24.7%.[92]

In 2021, by introducing neutral or weak donors of the trimethylbenzene unit, *m*-terphenyl unit, *p*-phenylcarbazole, and *m*-phenylcarbazole into the opposite position of the MR framework, four MR TADF emitters **162–165** are obtained by Lu *et al.* All of them successfully achieved λ values less than 0.12 eV and FWHM of about 0.11 eV (20 nm). The OLEDs based on **163** exhibited the EQE_{max} of 28.9% and the FWHM of 0.14 eV (28 nm).[93]

In 2021, Wang's group first combined circular-polarized luminescence (CPL) with MR-TADF to obtain the narrowband green CP-MR-TADF enantiomers, **166** and **167**. By grafting chiral (*R*/*S*)-octahydro-binaphthol ((*R*/*S*)-OBN) derivatives onto DtCzB-Bpin, CPEL signal, narrowband emission and TADF characteristics were obtained simultaneously. The OLEDs based on **166** and **167** showed EQE_{max} of 29.4% and 24.5% and FWHM of 30 and 33 nm. The EL asymmetry factor (g_{EL}) was $+1.43 \times 10^{-3}$/-1.27×10^{-3} and $+4.60 \times 10^{-4}$/-4.76×10^{-4}, respectively.[94]

Although MR-TADF materials possess outstanding advantages, they suffer from aggregation-induced quenching and efficiency roll-off in OLEDs due to their rigid plane structure and relatively low RISC. To solve these problems, in 2022, Duan *et al.* sterically wrapped MR dopants with a fluorescent MR core sandwiched by bulk substituents to address the intractable challenges by reducing intermolecular interactions.

The optimal emitter **168** realized remarkably high EQE_{max} of 36.3–37.2%, identical small FWHMs of 24 nm, and alleviated efficiency roll-offs in OLEDs.[95] Similarly, in the same year, by segregating the planar MR-TADF skeleton using two bulky carbazolyl units, a highly emissive molecule **169** with enhanced quenching resistance was reported by Yang *et al.* The steric effect largely removed the formation of detrimental excimers/aggregates, and boosted the performance of the corresponding device with an EQE_{max} up to 40.0% and FWHM of 25 nm. Even at a doping ratio of 30 wt%, the EQE_{max} was retained to be 33.3% with a nearly unchanged emission spectrum.[96] In 2022, Jiang *et al.* proposed a mono-substituted design strategy by introducing spiro-9,9′-bifluorene (SBF) unit with different substituted sites into the MR-TADF system for the first time, and MR-TADF compounds **170** and **171** were thus obtained. As a classic steric group, SBF with a spatial blocking effect could hinder interchromophore interactions without participating in the MR effect. **170** and **171** exhibited high EQE_{max} of 32.2 and 35.9% and narrow-band emission of $\sim$27 nm.[97] Further, two MR TADF molecules, **172** and **173**, were reported by Zheng *et al.* in 2023 by introducing the sterically hindered unit (*N*-phenylcarbazole) at the *para*- and *meta*-positions of the B/N framework. The face-to-face steric modulation between the non-conjugated benzene ring and B/N skeleton was achieved to separate adjacent MR-TADF skeletons and suppress self-quenching and spectral broadening. Consequently, **172** and **173**-based OLEDs showed an EQE_{max} of up to 33.6% and 32.6% with a FWHM of 26 and 30 nm, respectively.[98]

The relatively slow k_{RISC} ($<10^5$ S^{-1}) of MR-TADF devices commonly leads to the accumulation of triplet excitons in the emitter layer, resulting in serious efficiency roll-off. To address this issue, in 2022, You *et al.* put forward a "space-confined donor-acceptor (SCDA)" strategy to accelerate the RISC process. The introduction of SCDA units onto the MR-skeleton induced intermediate triplet states, which led to a multichannel RISC process and thus increased k_{RISC}. As illustrated examples, efficient MR-emitters **174** and **175** have been developed with a submicrosecond delayed lifetime and high k_{RISC} of 2.13×10^{6} s^{-1} and 1.55×10^{6} s^{-1}. The EQE_{max} and EQE at 1000 cd m^{-2} of **174** were up to 32.5% and 22.9%, respectively.[99]

In 2022, Che *et al.* described a simple gold(I) coordination strategy to enhance the spin–orbit coupling of green and blue BN(O)-based MR-TADF emitters, which resulted in a notable increase in the rate of the spectroscopically observed ISC process to 3×10^{9} s^{-1} with nearly unitary ISC quantum yield. The vapor-deposited ultrapure-green OLEDs fabricated with **176** emitter delivered a high luminance of up to 2.53×10^{5} cd m^{-2} as well as an EQE up to 30.3% with roll-offs as low as 0.8% and long device lifetimes (LT60) of 1210 h at 1000 cd m^{-2}.[100]

A new MR-TADF emitter **177** was developed by Yang *et al.* in 2022 through the coordination of Au with a B/N-embedded polycyclic ligand. Benefitting from the Au perturbation, the RISC rate was dramatically accelerated to 2.3×10^{7} s^{-1}, leading to a delayed fluorescence lifetime as short as 4.3 μs. The EQE_{max} of the **177** device was 35.8% and EQE remained at 32.3% at 10 000 cd m^{-2}.[101] Heavy-atom integration into the TADF molecule could significantly promote the RISC process. Subsequently, they further reported a pure green multi-resonance TADF molecule **178** and **179** by introducing a peripheral heavy atom selenium onto the parent BN-Cz molecule. The OLEDs based on **178** exhibited state-of-the-art performance with an EQE_{max} of 40.1%, a PE of 176.9 lm W^{-1}, well-suppressed efficiency roll-off and pure green gamut.[102]

In 2023, Zhang *et al.* incorporated the heavy atom effect *via* facilely hanging heavy atom-containing chains onto an MR framework and thus synthesized two MR emitters (sulfur ether group for **180** and sulfone group for **181**). k_{RISC} of **180** was increased to 1.40×10^{5} s^{-1} because of sufficient natural transition orbital (NTO) contributions from the heavy atom, compared to a relatively slow k_{RISC} of 5.6×10^{4} s^{-1} for **181**. OLEDs using **180** as the emitter showed an EQE_{max} of 30.0% and an alleviated efficiency roll-off of 44% at 1000 cd m^{-2}. In contrast, OLEDs based on **181** showed an EQE_{max} of 33.0% but a more severe efficiency $roll\text{-}off_{1000}$ of 65%.[103] In the same year, they also reported two MR-TADF emitters (**182** and **183**) *via* managing long- and short-range charge-transfer excitations to study the structure–property relationship. OLEDs based on **182** as the emitter achieved an EQE_{max} of 35.6% and an FWHM of 35 nm, in which short-range CT excitation was dominant in the S_1 excited state. In contrast, OLEDs based on **183** achieved an EQE_{max} of 27.2% and a broadened FWHM of 56 nm with an overloaded long-range CT excitation in the S_1 state.[104]

Extension of the conjugate skeleton of MR-TADF or introduction of heteroatoms into the MR skeleton is also a generally used method to finely modulate the emission color. In 2020, by fusing the difficult-to-access aza-aromatics onto B (boron)–N

(nitrogen) skeleton, a hybridized MR and charge transfer (HMCT) molecule **184** was successfully synthesized by Duan *et al.* through an effective one-shot multiple cyclization method. **184** showed pure green fluorescence with a PLQY of 99.7%. The corresponding green device exhibited an EQE_{max} of 28.2% and PE of 121.7 lm W^{-1}, respectively, with FWHM of merely 30 nm and CIE_y coordinate of 0.69, representing the purest green bottom-emitting OLEDs.[105]

In 2022, Zheng *et al.* achieved two π-extended MR-TADF emitters **185** and **186** *via* fusing conjugated high-triplet-energy units (carbazole, dibenzofuran) into the B/N framework, aiming to increase charge transfer delocalization of the B/N skeleton and minimize ΔE_{ST}. This strategy endowed the two emitters with FWHM of 27 and 29 nm, and high PLQYs above 90% in doped films, respectively. The devices of **185** and **186** showed emission peaks at 487 and 500 nm and an EQE_{max} of 26.1% and 28.0%, respectively.[106] They further reported two emitters **187** and **188** based on indolo[3,2,1-*jk*]carbazole unit and boron–nitrogen skeletons, whose emission peaks were located at 496 and 521 nm with a FWHM of 34 and 29 nm, respectively. Meanwhile, fast rate constants of RISC of above 10^6 s^{-1} were obtained due to small ΔE_{ST} and large SOC values. Notably, planar molecular structures along the transition dipole moment direction endowed them with high horizontal emitting dipole ratios of up to 94%. Consequently, the corresponding OLEDs of **187** and **188** showed the EQE_{max} of 31.7% and 32.2%, respectively. Particularly, OLEDs with **188** displayed ultra-pure green emission with CIE coordinates of (0.22, 0.71).[107]

Wang *et al.* proposed a novel MR-TADF molecular construction paradigm based on polycyclization of the MR parent core, and constructed a representative MR-PAH based on *para*-alignment boron and nitrogen atoms into a six-membered ring (*p*-BNR). The target model molecule **189** showed green fluorescence with an emission peak at 523 nm and a narrow FWHM of 34 nm. The OLED employing BN-TP as an emitter exhibited ultrapure green emission with CIE coordinates of (0.26, 0.70), and an EQE_{max} of 35.1%.[108] Later, based on the unique nitrogen-atom embedding molecular engineering (NEME) strategy, a series of compounds **190–193** have been customized by them. The nitrogen-atom anchored at different positions of the triphenylene hexagonal lattice entailed varying degrees of perturbation to the electronic structure. They demonstrated the precise regulation of emission maxima of MR-TADF emitters to meet the actual industrial demand, and further enormously enriched the MR-TADF molecular reservoir. The device based on **192** showed an FWHM of 33 nm, CIE coordinates of (0.23, 0.71), and an EQE_{max} of 37.3%.[109]

In 2022, Zhang *et al.* linked the outer phenyl groups in MR-type blue-emitting B/N molecules through bonding and spiro-carbon bridges, resulting in rigid green TADF emitters **194** and **195**. The MR effect and multiple interlocking strategies greatly suppressed the high-frequency vibrations in the molecules, which emitted green light with an FWHM of 14 nm and a CIE_y value of 0.77 in cyclohexane. Doping these emitters into a traditional green-emitting phosphorescence OLEDs endowed the device with a Broadcast Service Television 2020 color-gamut, 50% improved EQE, and an extremely high luminescence of 5.1×10^5 cd m^{-2}, making it the greenest and brightest OLED ever reported.[110]

In addition to extending the central benzene ring in the B/N skeleton, researchers also modified the carbazole unit of the blue-green molecule DtBuCzB to produce pure green emission of MR TADF derivatives. For example, in 2021, Yang *et al.* demonstrated **196** and **197** with a simple modification of the B/N framework by insertion of two sp^3 carbon atoms, which served as locks to rigidify the molecular backbone and also imposed a significant impact on the corresponding photophysical properties by extending the FMO to the appended phenyl units. **196** and **197** achieved EL peaks above 500 nm. The **197**-based device had an EQE_{max} of 28.2% and CIE coordinates of (0.21, 0.65).[111]

Kido *et al.* developed a novel one-pot borylation method that did not require the use of hazardous *tert*-BuLi in 2021. By inserting carbon and oxygen into the skeleton, two types of green-emitting MR-TADF emitters **198** and **199** were created. OLEDs using **198** and **199** exhibited the EQE_{max} of 20.3% and 23.3%, respectively, with FWHM values of 49 and 47 nm, respectively.[112]

In 2022, Yang *et al.* reported a series of heavy-atom incorporating emitters **200–202**, based on a sulfur or selenium-integrated B/N skeleton. **202** possessed a 100% PLQY and a high k_{RISC} of 2.0×10^6 s^{-1} because of the heavy atom effect of sulfur and selenium atoms. The corresponding green OLEDs exhibited EQE_{max} up to 36.8% and ultralow efficient roll-off (2.8% and 14.9% at 1000 cd m^{-2} and 10 000 cd m^{-2}, respectively).[123] Lu *et al.* designed asymmetric MR-TADF emitters **203** and **204**. These emitters could facilitate the RISC process because sulfur atoms could effectively enhance SOC through the heavy atom effect. A high PLQY of 96% and a fast k_{RISC} of above 1.0×10^5 s^{-1} were achieved in **204**. The corresponding OLEDs exhibited a pure green emission with an EQE_{max} of 32.8%, and EQE exceeded 23% at a high brightness of 1000 cd m^{-2}.[114] Another two asymmetric molecules, **205** and **206**, were realized by suppressing the shoulder peaks in the emission spectra of conventional PAHs by Duan *et al.* This method simultaneously improved molecular rigidity and reduced vibration frequency. The **205**-based device showed an FWHM of 21 nm, an EQE_{max} of 30.5%, and the CIE coordinate of (0.16, 0.77), which meet the green requirements of BT.2020.[115]

Compared to the peripheral modified chiral unit, several research groups have developed MR-TADF molecules with chiral characteristics. In 2022, Chou *et al.* successfully designed and synthesized a set of integrated CPMR-TADF molecules, (+)/(−)**207** and (+)/(−)**208**, using a strategy of asymmetric peripheral locking enantiomers. The devices based on (+)/(−)**207** and (+)/(−)**208** exhibited both TADF and CPL properties with FWHM of 49/50 nm and 48/47 nm, EQE_{max} of 20.6%/19.0% and 22.0%/26.5%, g_{EL} of $+3.7 \times 10^{-3}/-3.1 \times 10^{-3}$ and $+1.9 \times 10^{-3}/-1.6 \times 10^{-3}$, respectively.[116] Yang *et al.* also developed a pair of helicene-based enantiomers, (P/M) **209**, which merged helical chirality and the B/N/S inserted polycyclic aromatic framework to concurrently feature CPL and narrow TADF characteristics. Green CP-OLEDs based on enantiomers demonstrated an EQE_{max} of 31.5%/30.7%, an FWHM of 49/50 nm, and g_{EL} of $+1.2 \times 10^{-3}$ and -2.2×10^{-3}, respectively.[117] They further designed a pair of chiral green emitters, (*R*)/(*S*) **210**. CPL

properties came from the sp^3 hybridization of carbon atoms, which also locked the molecular geometry and improved the molecular rigidity. The OLEDs based on (*R*)/(*S*) **210** showed an EQE_{max} of 37.2%/36.1%, and g_{EL} of $+2.7 \times 10^{-4}/-2.9 \times 10^{-4}$, respectively.[118]

Introduction of two or more boron atoms into the MR skeleton also generated excellent narrowband green emitters. These MR TADF molecules are of two types depending on the position of the second B atom, that is, *meta* B–π–B and *para* B–π–B system. In 2020, Hatakeyama reported carbazole-based DABNA analogues from one-shot borylation. Under the optimized reaction conditions, the monoborylated and diborylated derivatives were selectively obtained in good yields. This facile and scalable method enabled the preparation of diverse CzDABNAs, which exhibited excellent TADF properties with small FWHMs and tuning of the emission wavelength from deep blue to green region. With the *meta* B–π–B and N–π–N structure, **211**-based OLEDs showed a green emission peak at 497 nm, an FWHM of 29 nm, and an EQE_{max} of 26.7%.[60] They also prepared a solution-processable MR-TADF material **212** with an extended π-skeleton and bulky substituents *via* a four-step process involving one-shot double borylation. Furthermore, to facilitate charge recombination, two novel semiconducting polymers with similar ionization potentials to that of **212** were synthesized for use as interlayer and emissive layers. These materials were used to fabricate a pure green OLED with CIE coordinates of (0.12, 0.63) and an EQE of 21.8%, representing the first solution-processed OLED featuring high color purity and efficiency.[119] Furthermore, they reported two MR-TADF emitters with similar structures, **213** and **214**. By introduction of cyano groups into the blue-emitting MR-TADF material (ν-DABNA), a remarkable bathochromic shift was induced without a loss of color purity. The OLEDs based on **213** displayed an emission peak at 504 nm, an FWHM of 23 nm, CIE coordinates of (0.13, 0.65), and an EQE_{max} of 31.9%.[120] Later, they demonstrated a sequential multiple borylation reaction that provided new synthetically accessible chemical space. **214**, the proof-of-concept material, exhibited narrowband green TADF with an FWHM of 22 nm and a small ΔE_{ST} of 13 meV. The OLEDs employing it as an active layer exhibited an EL peak at 512 nm, with CIE coordinates of (0.13, 0.73) and a high EQE_{max} of 31.1%. Moreover, the device showed minimum efficiency roll-off, with an EQE of 29.4% at 1000 cd m^{-2}.[121] Wang *et al.* reported a ternary B–O–N embedded PAH, **215**, by adopting the *para* boron–π–boron and *para* oxygen–π–oxygen strategy. **215** presented a vivid green emission with a high PLQY of 96% and an extremely narrow FWHM of 19 nm/0.09 eV, which surpassed all previously reported green TADF emitters to date. In addition, the long molecular structure along the transition dipole moment direction endowed it with a high horizontal emitting dipole ratio of 96%. **215**-based OLEDs revealed an emission peak at 504 nm and an FWHM of 24 nm/0.12 eV. The TADF-sensitized device realized an FWHM of 27 nm and an EQE_{max} of 37.1%.[122] Zheng *et al.* developed a simple strategy to achieve ternary B/N-based polycyclic heteroaromatic emitters from pure blue (463 nm) to yellow (553 nm) *via* tuning the coordination between B/N and heteroatom, aiming to increase charge transfer delocalization of the polycyclic heteroaromatic emitters and adjust photophysical properties. This strategy endowed the four emitters with FWHMs of 20–28 nm, respectively. Among these, **216–217** achieved FWHM of 20 nm and 28 nm and EQE_{max} of 26.7% and 21.8% in doped OLEDs, respectively.[123]

Over the last few years, huge progress has been made in the synthesis of green MR-TADF emitters for OLED applications. Compared to other colors, the definition of FWHM and the maximum emission wavelength is more stringent in green color, which creates a big challenge for ultrapure green emitters. In this section, green B/N-containing emitters possess maximum EL peaks between 490 and 560 nm. Green B/N-based TADF emitters containing DABNA units are summarized in Fig. 5 and Table 5.

2.3.3 Red B/N-based TADF emitters. According to the energy gap law, efficient red TADF emitters are rare, recognized as the fact that nonradiative transitions will significantly increase with the decreased energy gap. The development of B-based red MR TADF emitters is still a big challenge due to the limitation of electron-accepting moieties. Up to 2020, Yasuda *et al.* demonstrated that the strategic implementation of electron-accepting tricoordinate boron and electron-donating carbazole subunits into PAHs produced a family of attractive full-color luminophores with narrowband emission. Among these, **218** was the first narrowband red MR-TADF material, which showed a maximum PL emission of 615 nm and an FWHM of 21 nm. The devices with **218** as emitter achieved an EQE_{max} of 22.0% and CIE coordinates of (0.67, 0.33).[77]

The *para* D–π–D and A–π–A structures could improve the donor and acceptor strength, thus enhancing the intramolecular push-pull electron effect, which contributes to narrowing the energy gap. In 2021, Duan *et al.* developed two red MR compounds, **219** and **220**. The introduction of B-phenyl-B and N-phenyl-N structures enhanced the electronic coupling of those *para*-positioned atoms, gave rise to restricted p-bonds on the phenyl-core for delocalized excited states and generated a narrow energy gap. **219** and **220** achieved EL peaks at 662 and 692 nm, FWHM of 48 and 49 nm, and EQE_{max} of 28.1% and 27.6% in a normal planar OLED structure.[124]

In 2022, MR emitters **221** and **222** were designed and synthesized for narrowband red emission by embedding two pairs of S and N atoms and two B atoms in *para*-positions of central benzene rings within a tridecacyclic aromatic skeleton. 222 combined high PLQY of 85% and rapid k_{RISC} of 2.2×10^5 s^{-1}. Solution-processed correlated OLEDs realized a maximum emission of 641 nm, an FWHM of 39 nm, and an EQE_{max} of 7.8%.[125]

In 2022, Yang *et al.* reported a series of red MR emitters **223–225** by *para*-positioning N–π–N, O–π–O, B–π–B pairs onto a benzene ring to construct an MR central core. These emitters could be facilely and modularly synthesized, allowing for easy fine-tuning of emission spectra by peripheral groups. They displayed near-unity PLQY, a fast radiative decay rate up to 7.4×10^7 s^{-1}, and an FWHM of 32 nm. Pure red OLEDs based on **223** sensitized by phosphor realized state-of-the-art device performance with EQE exceeding 36%, ultra-low efficiency roll-

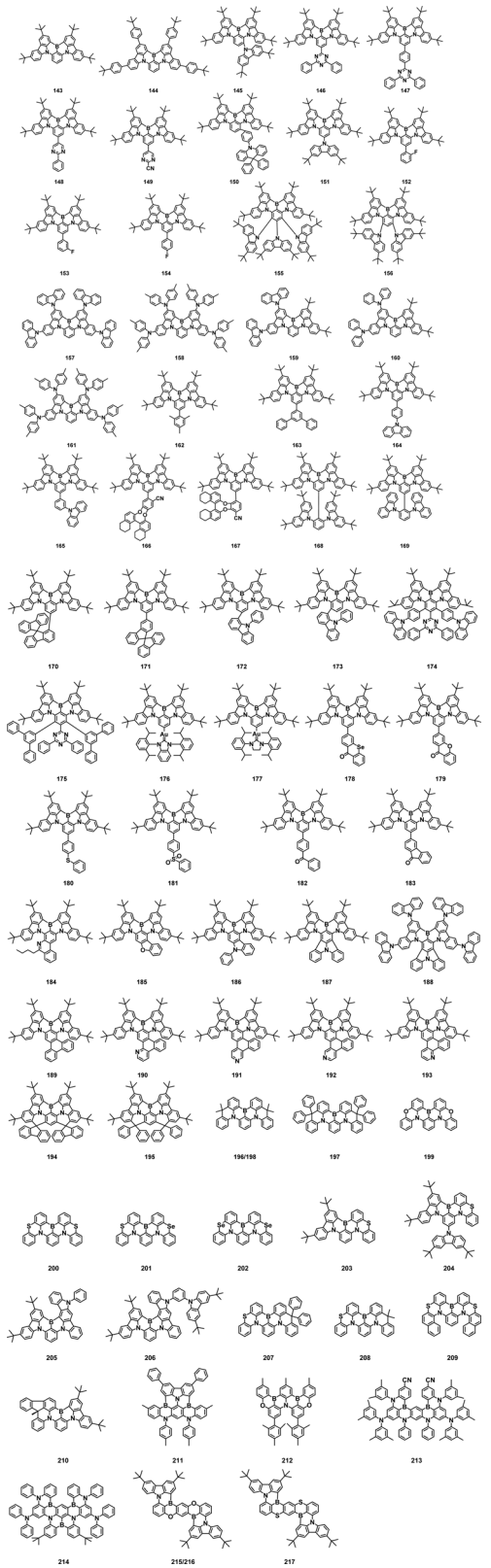

Fig. 5 Molecular structures of green B/N-based TADF emitters containing DABNA units.

off (EQE remains as high as 25.1% at the brightness of 50 000 cd m $^{-2}$), ultra-high brightness over 130 000 cd m^{-2}, together

Table 5 Summary of the performances of green B/N-based TADF emitters containing DABNA units

Compound	PLQY[a] [%]	λ_{PL}[b] [nm]	λ_{EL}[c] [nm]	ΔE_{ST}[d] [eV]	EQE_{max}[e] [%]	CIE[f] [x, y]	Ref.
143	91	481	488	0.13	21.6	0.10, 0.42	87
144	97	496	504	0.09	23.4	0.15, 0.61	87
145	97	519	528	0.08	31.4	0.26, 0.68	88
146	94	521	532	0.18	24.6	0.33, 0.63	89
147	97	501	516	0.11	29.8	0.18, 0.67	89
148	96	499	508	0.11	28.6	0.16, 0.66	89
149	93	515	540	0.15	25.0	0.35, 0.63	89
150	97	491	496	0.14	42.0	0.09, 0.54	90
151	—	477	474	—	18.9	0.13, 0.20	91
152	88.7	494	501	0.16	22.0	0.16, 0.60	91
153	83.4	499	499	0.08	22.7	0.20, 0.58	91
154	91.4	496	493	0.11	20.9	0.12, 0.48	91
155	90	517	515	0.14	31.8	0.26, 0.68	77
156	85	549	549	0.14	29.3	0.38, 0.61	77
157	89	517	514	0.09	29.2	0.16, 0.71	65
158	87	576	571	0.14	19.6	0.47, 0.51	65
159	99	496	506	0.11	24.3	0.15, 0.63	92
160	98	534	545	0.13	24.5	0.38, 0.61	92
161	98	562	568	0.09	24.7	0.47, 0.52	92
162	92	486	488	0.12	27.8	0.14, 0.36	93
163	94	492	492	0.09	28.9	0.10, 0.46	93
164	95	491	496	0.15	27.2	0.13, 0.54	93
165	88	495	496	0.14	25.9	0.15, 0.55	93
166	99	493	496	0.12	29.4	0.11, 0.52	94
167	96	500	508	0.13	24.5	0.14, 0.64	94
168	98	499	488	0.13	37.2	0.11, 0.43	95
169	93	490	496	0.13	40.0	0.09, 0.50	96
170	93	493	492	0.13	35.9	0.077, 0.471	97
171	90	493	496	0.15	32.2	0.092, 0.515	97
172	92	489	496	0.14	33.9	0.08, 0.52	98
173	95	502	500	0.09	32.6	0.10, 0.56	98
174	93	490	513	0.13	32.5	0.17, 0.68	99
175	95	492	513	0.11	31.4	0.16, 0.70	99
176	91	513	510	0.08	30.3	0.16, 0.68	100
177	95	514	520	0.07	35.8	0.16, 0.67	101
178	96	517	517	0.13	40.1	0.19, 0.70	102
179	93	515	516	0.08	37.3	0.19, 0.70	102
180	97.6	488	500	0.14	30.0	0.13, 0.60	103
181	98.1	498	512	0.14	33.0	0.17, 0.68	103
182	97.6	497	512	0.14	35.6	0.16, 0.68	104
183	75.3	516	544	0.09	27.2	0.37, 0.61	104
184	94	522	528	0.18	25.7	0.28, 0.69	105
185	92	457	502	0.12	28.0	0.12, 0.62	106
186	93	500	491	0.09	26.1	0.09, 0.41	106
187	98	496	499	0.06	31.7	0.14, 0.56	107
188	98	521	524	0.01	32.2	0.22, 0.71	107
189	96	524	528	0.14	35.1	0.26, 0.70	108
190	95	534	532	0.17	34.9	0.28, 0.69	109
191	91	535	534	0.19	31.9	0.30, 0.67	109
192	97	526	524	0.15	37.3	0.23, 0.71	109
193	97	530	528	0.14	36.5	0.27, 0.70	109
194	93	531	535	0.04	26.2	0.26, 0.72	110
195	98	523	527	0.04	29.3	0.21, 0.75	110
196	63	485	502	0.14	21.1	0.14, 0.54	111
197	86	490	504	0.11	28.2	0.14, 0.56	111
198	88	4841	503	0.16	20.3	0.18, 0.60	112
199	90	502	516	0.17	23.3	0.22, 0.67	112
200	68	525	520	0.13	34.6	—	113
201	86	520	515	0.12	35.7	—	113
202	95	514	512	0.14	36.8	—	113
203	91	510	520	0.11	27.6	0.26, 0.65	114
204	96	505	516	0.09	32.8	0.24, 0.63	114
205	99.2	521	523	0.22	30.5	0.22, 0.74	115
206	98.3	520	523	0.18	29.8	0.22, 0.74	115
207	88	500	510	0.14	20.6	0.186, 0.632	116
208	87	497	506	0.14	26.5	0.167, 0.603	116
(P)209	98	525	523	0.15	31.5	0.26, 0.66	117
(M)209	98	525	524	0.15	30.7	0.26, 0.66	117

Table 5 (*continued*)

Compound	PLQY[a] [%]	λ_{PL}[b] [nm]	λ_{EL}[c] [nm]	ΔE_{ST}[d] [eV]	EQE_{max}[e] [%]	CIE[f] [*x*, *y*]	Ref.
(R)210	96	497	504	0.11	37.2	0.12, 0.63	118
(S)210	96	497	503	0.11	36.1	0.12, 0.62	118
211	87	504	497	0.06	26.7	0.12, 0.57	60
212	71	506	505	0.12	21.8	0.12, 0.63	119
213	86	496	504	0.10	31.6	0.13, 0.65	120
214	87	509	512	0.013	31.1	0.13, 0.73	121
215	96	500	504	0.17	37.1	0.14, 0.53	122
216	98	505	510	0.13	26.7	0.17, 0.68	123
217	98	553	556	0.13	21.8	0.42, 0.57	123

[a] Photoluminescence quantum yield. [b] PL emission maximum. [c] EL emission maximum. [d] Singlet–triplet energy gap. [e] Maximum external EL quantum efficiency. [f] Maximum external quantum efficiency.

with good device lifetime. By roughly assuming a moderate acceleration factor of 1.7, the LT90 at 1000 and 100 cd m^{-2} was estimated to be as high as 1000 and 52 000 h for **223**-based devices.[126]

In 2023, Duan *et al.* designed and synthesized a narrowband pure-red MR emitter226 by fusing indolocarbazole segments into a B/O-embedded skeleton. The rigid indolocarbazole segment possessed a strong electron-donating ability due to its *para*-positioned nitrogen–π–nitrogen backbone and also enlarged the π-extension of the MR skeleton to suppress structural displacement during radiation, achieving concurrently red-shifted and narrowed emission spectrum. An emission maximum at 637 nm with an FWHM of merely 32 nm (0.097 eV) was recorded in toluene. The corresponding device simultaneously exhibited an EQE_{max} of 34.4% with low roll-off, CIE coordinates of (0.708, 0.292) precisely matching the standard of red BT.2020. An ultra-long lifetime of LT95 of $>10\,000$ h at 1000 cd m^{-2} was also obtained.[127]

In addition to the above design strategy, according to a large number of previous studies, it is found that expanding HOMO/

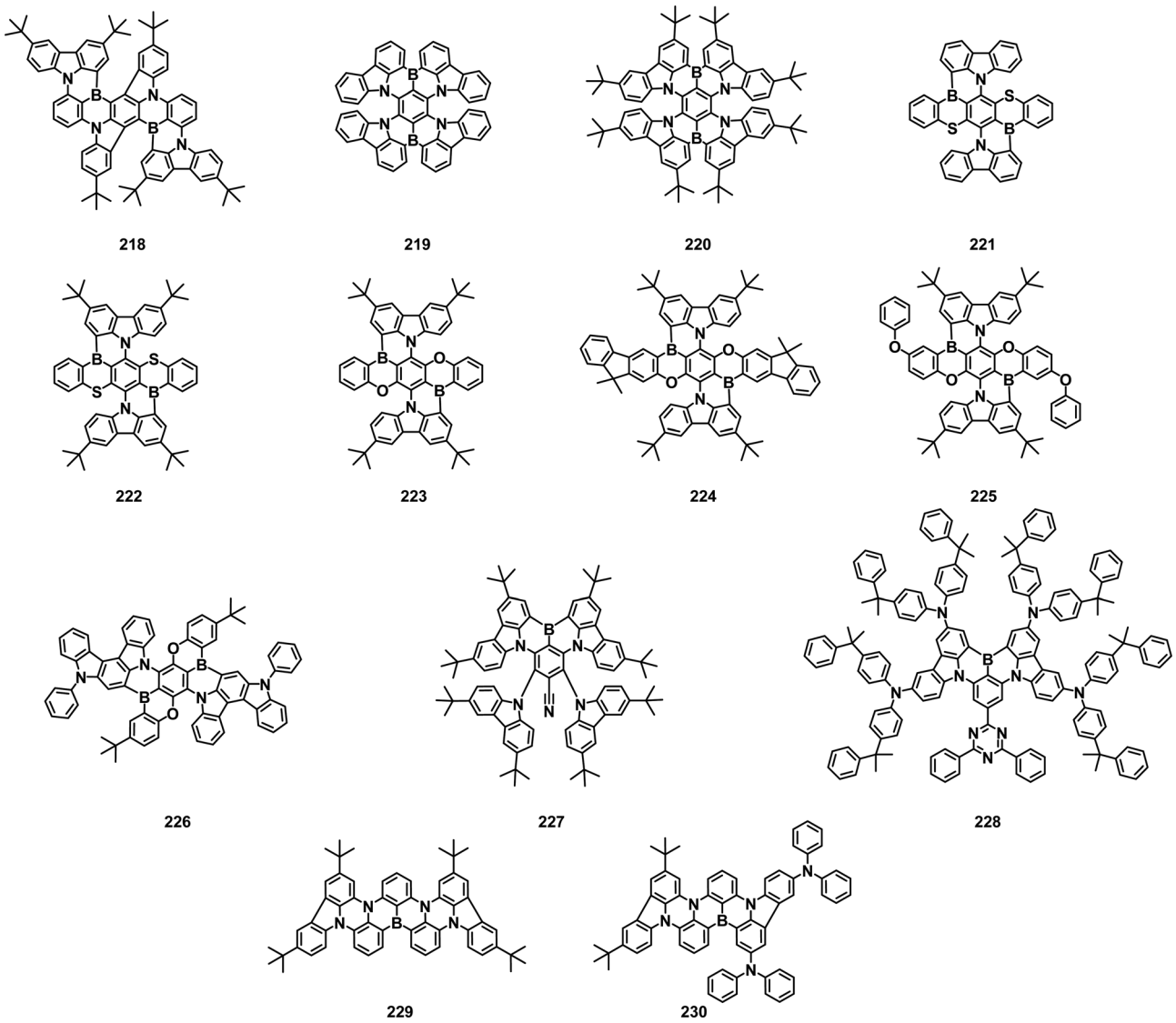

Fig. 6 Molecular structures of red B/N-based TADF emitters containing DABNA units.

Table 6 Summary of the performances of red B/N-based TADF emitters containing DABNA units

Compound	PLQY[a] [%]	λ_{PL}[b] [nm]	λ_{EL}[c] [nm]	ΔE_{ST}[d] [eV]	EQE_{max}[e] [%]	CIE[f] [x, y]	Ref.
218	89	615	616	0.19	22.0	0.67, 0.33	77
219	100	662	664	0.18	28.1	0.719, 0.280	124
220	100	692	686	0.16	27.6	0.721, 0.278	124
221	80	631	613	0.20	5.8	0.63, 0.35	125
222	85	641	616	0.19	7.8	0.65, 0.34	125
223	96	605	610	0.25	35.7	0.64, 0.34	126
224	95	609	618	0.27	34.4	0.65, 0.35	126
225	96	616	625	0.26	36.1	0.66, 0.34	126
226	95	637	643	0.09	34.4	0.708, 0.292	127
227	96	581	583	0.18	33.7	0.54, 0.46	128
228	94	624	617	0.11	22.0	0.654, 0.344	129
229	99	558	588	0.12	39.2	0.54, 0.44	130
230	95	583	584	0.06	32.4	0.54, 0.45	131

[a] Photoluminescence quantum yield. [b] PL emission maximum. [c] EL emission maximum. [d] Singlet–triplet energy gap. [e] Maximum external EL quantum efficiency. [f] Maximum external quantum efficiency.

LUMO distribution and improving π-conjugation can make the emission redshift. Alternatively, by introducing a donor or an acceptor into the position of HOMO or LUMO distribution of the MR skeleton, a red-shifted emission spectrum can also be realized. In 2021, an orange-red MR material, **227**, was reported by Bin *et al.* through the attachment of a CN functionality at the lowest unoccupied molecular orbital location of the MR-TADF skeleton which could promote attractive red-shifted emission owing to the exceptional electron-withdrawing capacity of the CN group. With the simultaneous introduction of CN and Cz groups to the blue emitting MR-TADF skeleton (BCz-BN), the emission wavelength was redshifted from 481 nm to 581 nm and the FWHM of 42 nm was maintained. The TADF-sensitized device showed EQE up to 33.7% and CIE coordinates of (0.54, 0.56).[128] In 2022, Wang *et al.* developed a pure red MR TADF molecule, **228**, by introducing auxiliary electron donor and acceptor moieties into the HOMO and LUMO distributed positions of the MR skeleton simultaneously. **228** exhibited a narrowband pure-red emission at 624 nm, with a high PLQY of 94% and a narrow bandwidth of 46 nm. Notably, the fabricated solution-processable pure-red OLED exhibited a state-of-the-art EQE over 20% with the CIE coordinates of (0.663, 0.337) and a long operational lifetime (LT50) of 1088 hours at an initial luminance of 1000 cd m^{-2}.[129] In 2022, Zhang group reported **229**, an orange-red MR molecule through modifying a prototypical MR core of DABNA by fusing carbazoles to the MR framework. **229** maintained the MR-dominated features of DABNA while red-shifting the emission. At the same time, the highly distorted structure could alleviate the aggregation quenching. Its OLED achieved an EQE_{max} of 39.2% at 588 nm and remained above 30.3% EQE even at high doping concentrations of 30 wt%.[130]

In 2023, Yang *et al.* proposed an effective method towards a long-wavelength MR-TADF emitter by integrating a strong electron-donating indolophenazine building block into the B/N-doped polycyclic aromatic hydrocarbons. The investigation of photophysical properties revealed that different electron-donating abilities had significant effects on luminescence features, including emission wavelength and FWHM. The device based on **230** as an emitter exhibited orange-red emission with an EL peak at 584 nm, an FWHM of 0.23 eV and an EQE_{max} of 32.4%.[131]

In this section, red-to-NIR emitters are defined as molecules that possess a maximum EL peak larger than 580 nm. Similar to yellow-orange MR-TADF emitters, red, deep-red and near-infrared emitters are still under development as the fact that nonradiative transitions will significantly increase with the decreased energy gap. This effect becomes even stronger for rigid and planar systems, such as in the nonradiative deactivation of PAHs. There still exists a formidable barrier to producing deep-red/near-infrared B/N-containing MR-TADF emitters with simultaneous narrow FWHM and high PLQYs. Red B/N-based TADF emitters containing DABNA units are listed in Fig. 6 and Table 6.

3. Conclusions and outlook

In conclusion, the photophysical properties of the representative boron-containing TADF materials including triaryl/diarylboron, 10*H*-phenoxaborin, DBNA, DABAN derivatives, and the performance of the corresponding OLEDs are summarized and analyzed systematically. OLEDs based on traditional TADF triaryl/diarylboron compounds have realized comparable, and even surpassed performance compared to state-of-the-art OLEDs adopting organometallic phosphorescent complexes. The broad emission spectra and poor color purity of organic light-emitting materials are one of the major challenges in their practical applications for many years. In this regard, organoboron-based MR-TADF emitters distinguish themselves from traditional D–A TADF materials and provide a potential solution for high-purity OLEDs. The MR-TADF materials with narrowband emission undoubtedly have become one of the most attractive and important projects for future ultrawide-color-gamut OLED displays meeting the B.T.2020 standard. Using a delicate molecular design strategy, the outstanding potential of MR-TADF materials, such as high color purity, color tunability from blue to red region, and excellent EL performance, has been unveiled. In particular, the B/N MR-TADF emitter can efficiently achieve the smallest FWHM reported so far. But many challenges remain in such MR-TADF emitters. Boron-based MR-TADF materials with deep blue and deep red emission are very limited. Further, the synthesis of boron-containing organic functional molecules is difficult, which commonly involves reagents such as butyl lithium and the reaction yields many by-products. Meanwhile, a wider chemical space beyond triangulene-type compounds and a deeper understanding of the design strategy for MR-TADF emitters are required. In addition, the efficiency roll-off and device stability is an issue still to be adequately addressed. Research efforts are needed to be devoted to the TADF system with a short lifetime and high k_{RISC} to minimize triplet-related exciton deactivation processes such as triplet-triplet

annihilation or singlet–triplet annihilation. Besides, how to achieve applications of the boron-containing narrowband TADF emitters in laser, biological imaging and other research fields remains unexplored. Although there are various factors ranging from materials to device engineering, it is believed that with the development of organoboron materials science, MR-TADF materials with narrow FWHM and high efficiency will continuously draw interest in both scientific research and industry, and make a significant contribution as a core technology for ultrawide-color-gamut OLED displays.

Conflicts of interest

There are no conflicts to declare.

Acknowledgements

This research is supported by the National Natural Science Foundation of China (22075100), the Jilin Provincial Science and Technology Department (No. 20220201082GX) and the Open Fund of the State Key Laboratory of Luminescence and Devices (South China University of Technology, No. 2021-skllmd).

Notes and references

1 N. N. Greenwood, Boron, *Comprehensive inorganic chemistry*, Pergamon Press, Oxford, 1973, pp. 665–993.
2 R. E. Krebs, *The history and use of our earth's chemical elements: a reference guide*, Greenwood Publishing Group, 2006.
3 B. Albert and H. Hillebrecht, Boron: elementary challenge for experimenters and theoreticians, *Angew. Chem., Int. Ed.*, 2009, **48**, 8640.
4 L. Butterwick, N. Oude and K. Raymond, Safety assessment of boron in aquatic and terrestrial environments, *Ecotoxicol. Environ. Saf.*, 1989, **17**, 339.
5 L. Ji, S. Griesbeck and T. B. Marder, Recent developments in and perspectives on three-coordinate boron materials: a bright future, *Chem. Sci.*, 2017, **8**, 846.
6 Z. M. Hudson and S. Wang, Metal-containing triarylboron compounds for optoelectronic applications, *Dalton Trans.*, 2011, **40**, 7805.
7 C. W. Tang and S. A. VanSlyke, Organic electroluminescent diodes, *Appl. Phys. Lett.*, 1987, **51**, 913.
8 S. Reineke, Complementary LED technologies, *Nat. Mater.*, 2015, **14**, 459.
9 B. Zhang, G. Tan, C. S. Lam, B. Yao, C. L. Ho, L. Liu, Z. Xie, W. Y. Wong, J. Ding and L. Wang, High-efficiency single emissive layer white organic light-emitting diodes based on solution-processed dendritic host and new orange-emitting iridium complex, *Adv. Mater.*, 2012, **24**, 1873.
10 H. Uoyama, K. Goushi, K. Shizu, H. Nomura and C. Adachi, Highly efficient organic light-emitting diodes from delayed fluorescence, *Nature*, 2012, **492**, 234.
11 Y. Tao, K. Yuan, T. Chen, P. Xu, H. Li, R. Chen, C. Zheng, L. Zhang and W. Huang, Thermally activated delayed fluorescence materials towards the breakthrough of organoelectronics, *Adv. Mater.*, 2014, **26**, 7931.
12 K. Matsuo and T. Yasuda, Boronate- and borinate-based pi-systems for blue thermally activated delayed fluorescence materials, *Chem. Commun.*, 2019, **55**, 2501.
13 Y. L. Rao and S. Wang, Four-coordinate organoboron compounds with a pi-conjugated chelate ligand for optoelectronic applications, *Inorg. Chem.*, 2011, **50**, 12263.
14 D. Li, H. Zhang and Y. Wang, Four-coordinate organoboron compounds for organic light-emitting diodes (OLEDs), *Chem. Soc. Rev.*, 2013, **42**, 8416.
15 E. von Grotthuss, A. John, T. Kaese and M. Wagner, Doping polycyclic aromatics with boron for superior performance in Materials Science and Catalysis, *Am. J. Org. Chem.*, 2018, **7**, 37.
16 T. Hatakeyama, K. Shiren, K. Nakajima, S. Nomura, S. Nakatsuka, K. Kinoshita, J. Ni, Y. Ono and T. Ikuta, Ultrapure blue thermally activated delayed fluorescence molecules: efficient HOMO-LUMO separation by the multiple resonance effect, *Adv. Mater.*, 2016, **28**, 2777.
17 A. Endo, K. Sato, K. Yoshimura, T. Kai, A. Kawada, H. Miyazaki and C. Adachi, Efficient up-conversion of triplet excitons into a singlet state and its application for organic light emitting diodes, *Appl. Phys. Lett.*, 2011, **98**, 083302.
18 K. Suzuki, S. Kubo, K. Shizu, T. Fukushima, A. Wakamiya, Y. Murata, C. Adachi and H. Kaji, Triarylboron-based fluorescent organic light-emitting diodes with external quantum efficiencies exceeding 20%, *Angew. Chem., Int. Ed.*, 2015, **54**, 15231.
19 Y. Liu, G. Xie, K. Wu, Z. Luo, T. Zhou, X. Zeng, J. Yu, S. Gong and C. Yang, Boosting reverse intersystem crossing by increasing donors in triarylboron/phenoxazine hybrids: TADF emitters for high-performance solution-processed OLEDs, *J. Mater. Chem. C*, 2016, **4**, 4402.
20 Y. H. Lee, S. Park, J. Oh, J. W. Shin, J. Jung, S. Yoo and M. H. Lee, Rigidity-induced delayed fluorescence by *ortho* donor-appended triarylboron compounds: record-high efficiency in pure blue fluorescent organic light-emitting diodes, *ACS Appl. Mater. Interfaces*, 2017, **9**, 24035.
21 X. L. Chen, J. H. Jia, R. Yu, J. Z. Liao, M. X. Yang and C. Z. Lu, Combining charge-transfer pathways to achieve unique thermally activated delayed fluorescence emitters for high-performance solution-processed, non-doped blue OLEDs, *Angew. Chem., Int. Ed.*, 2017, **56**, 15006.
22 Y. H. Lee, S. Park, J. Oh, S.-J. Woo, A. Kumar, J.-J. Kim, J. Jung, S. Yoo and M. H. Lee, High-efficiency sky blue to ultradeep blue thermally activated delayed fluorescent diodes based on *ortho*-carbazole-appended triarylboron emitters: above 32% external quantum efficiency in blue devices, *Adv. Opt. Mater.*, 2018, **6**, 1800385.
23 C.-C. Tsai, W.-C. Huang, H.-Y. Chih, Y.-C. Hsh, C.-W. Liao, C.-H. Lin, Y.-X. Kang, C.-H. Chang, Y. J. Chang and C.-W. Lu, Efficient donor-acceptor-donor borylated compounds with extremely small ΔE_{ST} for thermally activated delayed fluorescence OLEDs, *Org. Electron.*, 2018, **63**, 166.

24 Y. Liu, H. Huang, T. Zhou, K. Wu, M. Zhu, J. Yu, G. Xie and C. Yang, Boosting photoluminescence quantum yields of triarylboron/phenoxazine hybrids via incorporation of cyano groups and their applications as TADF emitters for high-performance solution-processed OLEDs, *J. Mater. Chem. C*, 2019, **7**, 4778.

25 C. Qu, G. Xia, Y. Xu, Y. Zhu, J. Liang, H. Zhang, J. Wang, Z. Zhang and Y. Wang, Boron-containing D–A–A type TADF materials with tiny singlet–triplet energy splittings and high photoluminescence quantum yields for highly efficient OLEDs with low efficiency roll-offs, *J. Mater. Chem. C*, 2020, **8**, 3846.

26 P. Ganesan, D.-G. Chen, W.-C. Chen, P. Gnanasekaran, J.-A. Lin, C.-Y. Huang, M.-C. Chen, C.-S. Lee, P.-T. Chou and Y. Chi, Methoxy substituents activated carbazole-based boron dimesityl TADF emitters, *J. Mater. Chem. C*, 2020, **8**, 4780.

27 A. Kumar, W. Lee, T. Lee, J. Jung, S. Yoo and M. H. Lee, Triarylboron-based TADF emitters with perfluoro substituents: high-efficiency OLEDs with a power efficiency over 100 lm W^{-1}, *J. Mater. Chem. C*, 2020, **8**, 4253.

28 Q. Chen, Y. Xiang, X. Yin, K. Hu, Y. Li, X. Cheng, Y. Liu, G. Xie and C. Yang, Highly efficient blue TADF emitters incorporating bulky acridine moieties and their application in solution-processed OLEDs, *Dyes Pigm.*, 2021, **188**, 109157.

29 G. Xia, C. Qu, Y. Zhu, J. Ye, K. Ye, Z. Zhang and Y. Wang, A TADF emitter featuring linearly arranged spiro-donor and spiro-acceptor groups: efficient nondoped and doped deep-blue OLEDs with CIE(y) <0.1, *Angew. Chem., Int. Ed.*, 2021, **60**, 9598.

30 Y. H. Lee, W. Lee, T. Lee, D. Lee, J. Jung, S. Yoo and M. H. Lee, Blue TADF emitters based on B-heterotriangulene acceptors for highly efficient OLEDs with reduced efficiency roll-off, *ACS Appl. Mater. Interfaces*, 2021, **13**, 45778.

31 J. Wang, N. Li, Q. Chen, Y. Xiang, X. Zeng, S. Gong, Y. Zou and Y. Liu, Triarylboron-cored multi-donors TADF emitter with high horizontal dipole orientation ratio achieving high performance OLEDs with near 39% external quantum efficiency and small efficiency Roll-off, *Chem. Eng. J.*, 2022, **450**, 137805.

32 M. Numata, T. Yasuda and C. Adachi, High efficiency pure blue thermally activated delayed fluorescence molecules having 10H-phenoxaborin and acridan units, *Chem. Commun.*, 2015, **51**, 9443.

33 Y. Kitamoto, T. Namikawa, D. Ikemizu, Y. Miyata, T. Suzuki, H. Kita, T. Sato and S. Oi, Light blue and green thermally activated delayed fluorescence from 10H-phenoxaborin-derivatives and their application to organic light-emitting diodes, *J. Mater. Chem. C*, 2015, **3**, 9122.

34 I. S. Park, K. Matsuo, N. Aizawa and T. Yasuda, High-performance dibenzoheteraborin-based thermally activated delayed fluorescence emitters: molecular architectonics for concurrently achieving narrowband emission and efficient triplet-singlet spin conversion, *Adv. Funct. Mater.*, 2018, **28**, 1802031.

35 D. H. Ahn, H. Lee, S. W. Kim, D. Karthik, J. Lee, H. Jeong, J. Y. Lee and J. H. Kwon, Highly twisted donor–acceptor boron emitter and high triplet host material for highly efficient blue thermally activated delayed fluorescent device, *ACS Appl. Mater. Interfaces*, 2019, **11**, 14909.

36 K. Matsuo and T. Yasuda, Blue thermally activated delayed fluorescence emitters incorporating acridan analogues with heavy group 14 elements for high-efficiency doped and non-doped OLEDs, *Chem. Sci.*, 2019, **10**, 10687.

37 T. Agou, K. Matsuo, R. Kawano, I. S. Park, T. Hosoya, H. Fukumoto, T. Kubota, Y. Mizuhata, N. Tokitoh and T. Yasuda, Pentacyclic ladder-heteraborin emitters exhibiting high-efficiency blue thermally activated delayed fluorescence with an ultrashort emission lifetime, *ACS Mater. Lett.*, 2019, **2**, 28.

38 H. Hirai, K. Nakajima, S. Nakatsuka, K. Shiren, J. Ni, S. Nomura, T. Ikuta and T. Hatakeyama, One-step borylation of 1,3-diaryloxybenzenes towards efficient materials for organic light-emitting diodes, *Angew. Chem., Int. Ed.*, 2015, **54**, 13581.

39 G. Meng, X. Chen, X. Wang, N. Wang, T. Peng and S. Wang, Isomeric bright sky-blue TADF emitters based on bisacridine decorated DBNA: impact of donor locations on luminescent and electroluminescent properties, *Adv. Opt. Mater.*, 2019, **7**, 1900130.

40 D. H. Ahn, S. W. Kim, H. Lee, I. J. Ko, D. Karthik, J. Y. Lee and J. H. Kwon, Highly efficient blue thermally activated delayed fluorescence emitters based on symmetrical and rigid oxygen-bridged boron acceptors, *Nat. Photonics*, 2019, **13**, 540.

41 D. H. Ahn, J. H. Maeng, H. Lee, H. Yoo, R. Lampande, J. Y. Lee and J. H. Kwon, Rigid oxygen-bridged boron-based blue thermally activated delayed fluorescence emitter for organic light-emitting diode: approach towards satisfying high efficiency and long lifetime together, *Adv. Opt. Mater.*, 2020, **8**, 2000102.

42 H. J. Kim, M. Godumala, S. K. Kim, J. Yoon, C. Y. Kim, H. Park, J. H. Kwon, M. J. Cho and D. H. Choi, Color-tunable boron-based emitters exhibiting aggregation-induced emission and thermally activated delayed fluorescence for efficient solution-processable nondoped deep-blue to sky-blue OLEDs, *Adv. Opt. Mater.*, 2020, **8**, 1902175.

43 H. Lim, H. J. Cheon, S. J. Woo, S. K. Kwon, Y. H. Kim and J. J. Kim, Highly efficient deep-blue OLEDs using a TADF emitter with a narrow emission spectrum and high horizontal emitting dipole ratio, *Adv. Mater.*, 2020, **32**, e2004083.

44 R. Braveenth, H. Lee, J. D. Park, K. J. Yang, S. J. Hwang, K. R. Naveen, R. Lampande and J. H. Kwon, Achieving narrow FWHM and high EQE over 38% in blue OLEDs using rigid heteroatom-based deep blue TADF sensitized host, *Adv. Funct. Mater.*, 2021, **31**, 2105805.

45 J. Hwang, H. Kang, J.-E. Jeong, H. Y. Woo, M. J. Cho, S. Park and D. H. Choi, Donor engineered deep-blue emitters for tuning luminescence mechanism in solution-processed OLEDs, *Chem. Eng. J.*, 2021, **416**, 129185.

46 T. Hua, Y.-C. Liu, C.-W. Huang, N. Li, C. Zhou, Z. Huang, X. Cao, C.-C. Wu and C. Yang, High-efficiency and low roll-off deep-blue OLEDs enabled by thermally activated delayed fluorescence emitter with preferred horizontal dipole orientation, *Chem. Eng. J.*, 2022, **433**, 133598.
47 R. Pei, H. Liu, C. Zhou, J. Miao and C. Yang, Efficient blue thermally activated delayed fluorescent emitters based on a boranaphtho[3,2,1-*de*]anthracene acceptor, *J. Mater. Chem. C*, 2021, **9**, 17136.
48 Y. Lee and J. I. Hong, High-efficiency thermally activated delayed fluorescence emitters with high horizontal orientation and narrow deep-blue emission, *Adv. Opt. Mater.*, 2021, **9**, 2100406.
49 J. Wang, J. Miao, C. Jiang, S. Luo, C. Yang and K. Li, Engineering intramolecular π-stacking interactions of through-space charge-transfer TADF emitters for highly efficient OLEDs with improved color purity, *Adv. Opt. Mater.*, 2022, **10**, 2201071.
50 D. Karthik, Y. H. Jung, H. Lee, S. Hwang, B. M. Seo, J. Y. Kim, C. W. Han and J. H. Kwon, Acceptor-donor-acceptor-type Orange-red thermally activated delayed fluorescence materials realizing external quantum efficiency over 30% with low efficiency roll-off, *Adv. Mater.*, 2021, **33**, e2007724.
51 X. Liang, Z. P. Yan, H. B. Han, Z. G. Wu, Y. X. Zheng, H. Meng, J. L. Zuo and W. Huang, Peripheral amplification of multi-resonance induced thermally activated delayed fluorescence for highly efficient OLEDs, *Angew. Chem., Int. Ed.*, 2018, **57**, 11316.
52 S. H. Han, J. H. Jeong, J. W. Yoo and J. Y. Lee, Ideal blue thermally activated delayed fluorescence emission assisted by a thermally activated delayed fluorescence assistant dopant through a fast reverse intersystem crossing mediated cascade energy transfer process, *J. Mater. Chem. C*, 2019, **7**, 3082.
53 J. H. Kim, W. J. Chung, J. Kim and J. Y. Lee, Concentration quenching–resistant multiresonance thermally activated delayed fluorescence emitters, *Mater. Today Energy*, 2021, **21**, 100792.
54 J. Park, K. J. Kim, J. Lim, T. Kim and J. Y. Lee, High efficiency of over 25% and long device lifetime of over 500 h at 1000 nit in blue fluorescent organic light-emitting diodes, *Adv. Mater.*, 2022, **34**, e2108581.
55 Y. Wang, Y. Duan, R. Guo, S. Ye, K. Di, W. Zhang, S. Zhuang and L. Wang, A periphery cladding strategy to improve the performance of narrowband emitters, achieving deep-blue OLEDs with CIEy <0.08 and external quantum efficiency approaching 20%, *Org. Electron.*, 2021, **97**, 106275.
56 H. J. Cheon, Y. S. Shin, N. H. Park, J. H. Lee and Y. H. Kim, Boron-based multi-resonance TADF emitter with suppressed intermolecular interaction and isomer formation for efficient pure blue OLEDs, *Small*, 2022, **18**, e2107574.
57 H. J. Cheon, S. J. Woo, S. H. Baek, J. H. Lee and Y. H. Kim, Dense local triplet states and steric shielding of a multi-resonance TADF emitter enable high-performance deep-blue OLEDs, *Adv. Mater.*, 2022, **34**, e2207416.
58 S. Xu, Q. Yang, Y. Zhang, H. Li, Q. Xue, G. Xie, M. Gu, J. Jin, L. Huang and R. Chen, Solution-processed multi-resonance organic light-emitting diodes with high efficiency and narrowband emission, *Chin. Chem. Lett.*, 2021, **32**, 1372.
59 Y. T. Lee, C. Y. Chan, M. Tanaka, M. Mamada, U. Balijapalli, Y. Tsuchiya, H. Nakanotani, T. Hatakeyama and C. Adachi, Investigating HOMO energy levels of terminal emitters for realizing high-brightness and stable TADF-assisted fluorescence organic light-emitting diodes, *Adv. Electron. Mater.*, 2021, **7**, 2001090.
60 S. Oda, W. Kumano, T. Hama, R. Kawasumi, K. Yoshiura and T. Hatakeyama, Carbazole-based DABNA analogues as highly efficient thermally activated delayed fluorescence materials for narrowband organic light-emitting diodes, *Angew. Chem., Int. Ed.*, 2021, **60**, 2882.
61 Y. Qiu, H. Xia, J. Miao, Z. Huang, N. Li, X. Cao, J. Han, C. Zhou, C. Zhong and C. Yang, Narrowing the electroluminescence spectra of multiresonance emitters for high-performance blue OLEDs by a peripheral decoration strategy, *ACS Appl. Mater. Interfaces*, 2021, **13**, 59035.
62 X. Lv, J. Miao, M. Liu, Q. Peng, C. Zhong, Y. Hu, X. Cao, H. Wu, Y. Yang, C. Zhou, J. Ma, Y. Zou and C. Yang, Extending the pi-skeleton of multi-resonance TADF materials towards high-efficiency narrowband deep-blue emission, *Angew. Chem., Int. Ed.*, 2022, **61**, e202201588.
63 Y. Wang, K. Di, Y. Duan, R. Guo, L. Lian, W. Zhang and L. Wang, The selective regulation of borylation site based on one-shot electrophilic C–H borylation reaction, achieving highly efficient narrowband organic light-emitting diodes, *Chem. Eng. J.*, 2022, **431**, 133221.
64 J. Bian, S. Chen, L. Qiu, R. Tian, Y. Man, Y. Wang, S. Chen, J. Zhang, C. Duan, C. Han and H. Xu, Ambipolar self-host functionalization accelerates blue multi-resonance thermally activated delayed fluorescence with internal quantum efficiency of 100%, *Adv. Mater.*, 2022, **34**, e2110547.
65 M. Yang, S. Shikita, H. Min, I. S. Park, H. Shibata, N. Amanokura and T. Yasuda, Wide-range color tuning of narrowband emission in multi-resonance organoboron delayed fluorescence materials through rational imine/amine functionalization, *Angew. Chem., Int. Ed.*, 2021, **60**, 23142.
66 J. Park, J. Lim, J. H. Lee, B. Jang, J. H. Han, S. S. Yoon and J. Y. Lee, Asymmetric blue multiresonance TADF emitters with a narrow emission band, *ACS Appl. Mater. Interfaces*, 2021, **13**, 45798.
67 J. Han, Z. Huang, X. Lv, J. Miao, Y. Qiu, X. Cao and C. Yang, Simple molecular design strategy for multiresonance induced TADF emitter: highly efficient deep blue to blue electroluminescence with high color purity, *Adv. Opt. Mater.*, 2021, **10**, 2102092.
68 T. Hua, J. Miao, H. Xia, Z. Huang, X. Cao, N. Li and C. Yang, Sulfone-incorporated multi-resonance TADF emitter for high-performance narrowband blue OLEDs with EQE of 32%, *Adv. Funct. Mater.*, 2022, **32**, 2201032.
69 J. Liu, L. Chen, X. Wang, Q. Yang, L. Zhao, C. Tong, S. Wang, S. Shao and L. Wang, Multiple resonance

dendrimers containing boron, oxygen, nitrogen-doped polycyclic aromatic emitters for narrowband blue-emitting solution-processed OLEDs, *Macromol. Rapid Commun.*, 2022, **43**, e2200079.

70 Q. Li, Y. Wu, Q. Yang, S. Wang, S. Shao and L. Wang, Selenium-doped polycyclic aromatic hydrocarbon multiresonance emitters with fast reverse intersystem crossing for narrowband blue emission, *ACS Appl. Mater. Interfaces*, 2022, **14**, 49995.

71 Q. Li, Y. Wu, X. Wang, Q. Yang, J. Hu, R. Zhong, S. Shao and L. Wang, Boron-, sulfur- and nitrogen-doped polycyclic aromatic hydrocarbon multiple resonance emitters for narrow-band blue emission, *Chem. – Eur. J.*, 2022, **28**, e202104214.

72 K. Matsui, S. Oda, K. Yoshiura, K. Nakajima, N. Yasuda and T. Hatakeyama, One-shot multiple borylation toward BN-doped nanographenes, *J. Am. Chem. Soc.*, 2018, **140**, 1195.

73 S. Oda, B. Kawakami, R. Kawasumi, R. Okita and T. Hatakeyama, Multiple resonance effect-induced sky-blue thermally activated delayed fluorescence with a narrow emission band, *Org. Lett.*, 2019, **21**, 9311.

74 Y. Kondo, K. Yoshiura, S. Kitera, H. Nishi, S. Oda, H. Gotoh, Y. Sasada, M. Yanai and T. Hatakeyama, Narrowband deep-blue organic light-emitting diode featuring an organoboron-based emitter, *Nat. Photonics*, 2019, **13**, 678.

75 H. Tanaka, S. Oda, G. Ricci, H. Gotoh, K. Tabata, R. Kawasumi, D. Beljonne, Y. Olivier and T. Hatakeyama, Hypsochromic shift of multiple-resonance-induced thermally activated delayed fluorescence by oxygen atom incorporation, *Angew. Chem., Int. Ed.*, 2021, **60**, 17910.

76 I. S. Park, M. Yang, H. Shibata, N. Amanokura and T. Yasuda, Achieving ultimate narrowband and ultrapure blue organic light-emitting diodes based on polycycloheteraborin multi-resonance delayed-fluorescence emitters, *Adv. Mater.*, 2022, **34**, e2107951.

77 M. Yang, I. S. Park and T. Yasuda, Full-color, narrowband, and high-efficiency electroluminescence from boron and carbazole embedded polycyclic heteroaromatics, *J. Am. Chem. Soc.*, 2020, **142**, 19468.

78 M. Nagata, H. Min, E. Watanabe, H. Fukumoto, Y. Mizuhata, N. Tokitoh, T. Agou and T. Yasuda, Fused-nonacyclic multi-resonance delayed fluorescence emitter based on ladder-thiaborin exhibiting narrowband sky-blue emission with accelerated reverse intersystem crossing, *Angew. Chem., Int. Ed.*, 2021, **60**, 20280.

79 J. A. Knoller, G. Meng, X. Wang, D. Hall, A. Pershin, D. Beljonne, Y. Olivier, S. Laschat, E. Zysman-Colman and S. Wang, Intramolecular borylation via sequential B-Mes bond cleavage for the divergent synthesis of B,N,B-doped benzo[4]helicenes, *Angew. Chem., Int. Ed.*, 2020, **59**, 3156.

80 X. Wang, Y. Zhang, H. Dai, G. Li, M. Liu, G. Meng, X. Zeng, T. Huang, L. Wang, Q. Peng, D. Yang, D. Ma, D. Zhang and L. Duan, Mesityl-functionalized multi-resonance organoboron delayed fluorescent frameworks with wide-range color tunability for narrowband OLEDs, *Angew. Chem., Int. Ed.*, 2022, **61**, e202206916.

81 K. Rayappa Naveen, H. Lee, R. Braveenth, K. Joon Yang, S. Jae Hwang and J. Hyuk Kwon, Deep blue diboron embedded multi-resonance thermally activated delayed fluorescence emitters for narrowband organic light emitting diodes, *Chem. – Eur. J.*, 2022, **432**, 134381.

82 K. R. Naveen, H. Lee, L. H. Seung, Y. H. Jung, C. P. Keshavananda Prabhu, S. Muruganantham and J. H. Kwon, Modular design for constructing narrowband deep-blue multiresonant thermally activated delayed fluorescent emitters for efficient organic light emitting diodes, *Chem. – Eur. J.*, 2023, **451**, 138498.

83 S. M. Suresh, E. Duda, D. Hall, Z. Yao, S. Bagnich, A. M. Z. Slawin, H. Bassler, D. Beljonne, M. Buck, Y. Olivier, A. Kohler and E. Zysman-Colman, A deep blue B,N-doped heptacene emitter that shows both thermally activated delayed fluorescence and delayed fluorescence by triplet-triplet annihilation, *J. Am. Chem. Soc.*, 2020, **142**, 6588.

84 K. Stavrou, S. Madayanad Suresh, D. Hall, A. Danos, N. A. Kukhta, A. M. Z. Slawin, S. Warriner, D. Beljonne, Y. Olivier, A. Monkman and E. Zysman-Colman, Emission and absorption tuning in TADF B,N-doped heptacenes: toward ideal-blue hyperfluorescent OLEDs, *Adv. Opt. Mater.*, 2022, **10**, 2200688.

85 S. Oda, B. Kawakami, Y. Yamasaki, R. Matsumoto, M. Yoshioka, D. Fukushima, S. Nakatsuka and T. Hatakeyama, One-shot synthesis of expanded heterohelicene exhibiting narrowband thermally activated delayed fluorescence, *J. Am. Chem. Soc.*, 2022, **144**, 106.

86 S. Oda, B. Kawakami, M. Horiuchi, Y. Yamasaki, R. Kawasumi and T. Hatakeyama, Ultra-narrowband blue multi-resonance thermally activated delayed fluorescence materials, *Adv. Sci.*, 2022, **10**, e2205070.

87 Y. Xu, Z. Cheng, Z. Li, B. Liang, J. Wang, J. Wei, Z. Zhang and Y. Wang, Molecular-structure and device-configuration optimizations toward highly efficient green electroluminescence with narrowband emission and high color purity, *Adv. Opt. Mater.*, 2020, **8**, 1902142.

88 Y. Xu, C. Li, Z. Li, Q. Wang, X. Cai, J. Wei and Y. Wang, Constructing charge-transfer excited states based on frontier molecular orbital engineering: narrowband green electroluminescence with high color purity and efficiency, *Angew. Chem., Int. Ed.*, 2020, **59**, 17442.

89 Y. Xu, C. Li, Z. Li, J. Wang, J. Xue, Q. Wang, X. Cai and Y. Wang, Highly efficient electroluminescent materials with high color purity based on strong acceptor attachment onto B–N-containing multiple resonance frameworks, *CCS Chem.*, 2022, **4**, 2065.

90 Q. Wang, Y. Xu, T. Yang, J. Xue and Y. Wang, Precise functionalization of a multiple-resonance framework: constructing narrowband organic electroluminescent materials with external quantum efficiency over 40%, *Adv. Mater.*, 2023, **35**, e2205166.

91 Y. Zhang, D. Zhang, J. Wei, Z. Liu, Y. Lu and L. Duan, Multi-resonance induced thermally activated delayed fluorophores for narrowband green OLEDs, *Angew. Chem., Int. Ed.*, 2019, **58**, 16912.

92 Y. Qi, W. Ning, Y. Zou, X. Cao, S. Gong and C. Yang, Peripheral decoration of multi-resonance molecules as a versatile approach for simultaneous long-wavelength and narrowband emission, *Adv. Funct. Mater.*, 2021, **31**, 2102017.

93 F. Liu, Z. Cheng, L. Wan, Z. Feng, H. Liu, H. Jin, L. Gao, P. Lu and W. Yang, Highly efficient multi-resonance thermally activated delayed fluorescence material with a narrow full width at half-maximum of 0.14 eV, *Small*, 2022, **18**, e2106462.

94 Y. Xu, Q. Wang, X. Cai, C. Li and Y. Wang, Highly efficient electroluminescence from narrowband green circularly polarized multiple resonance thermally activated delayed fluorescence enantiomers, *Adv. Mater.*, 2021, **33**, e2100652.

95 Y. Zhang, J. Wei, D. Zhang, C. Yin, G. Li, Z. Liu, X. Jia, J. Qiao and L. Duan, Sterically wrapped multiple resonance fluorophors for suppression of concentration quenching and spectrum broadening, *Angew. Chem., Int. Ed.*, 2022, **61**, e202113206.

96 P. Jiang, J. Miao, X. Cao, H. Xia, K. Pan, T. Hua, X. Lv, Z. Huang, Y. Zou and C. Yang, Quenching-resistant multi-resonance TADF emitter realizes 40% external quantum efficiency in narrowband electroluminescence at high doping level, *Adv. Mater.*, 2022, **34**, e2106954.

97 Y. K. Qu, D. Y. Zhou, F. C. Kong, Q. Zheng, X. Tang, Y. H. Zhu, C. C. Huang, Z. Q. Feng, J. Fan, C. Adachi, L. S. Liao and Z. Q. Jiang, Steric modulation of spiro structure for highly efficient multiple resonance emitters, *Angew. Chem., Int. Ed.*, 2022, **61**, e202201886.

98 X. F. Luo, H. X. Ni, X. Liang, D. Yang, D. Ma, Y. X. Zheng and J. L. Zuo, Face-to-face steric modulation to achieve high performance multiple-resonance thermally activated delayed fluorescence emitters with quenching resistant effect, *Adv. Opt. Mater.*, 2023, **11**, 2203002.

99 Y. Liu, X. Xiao, Z. Huang, D. Yang, D. Ma, J. Liu, B. Lei, Z. Bin and J. You, Space-confined donor-acceptor strategy enables fast spin-flip of multiple resonance emitters for suppressing efficiency roll-off, *Angew. Chem., Int. Ed.*, 2022, **61**, e202210210.

100 S. Cai, G. S. M. Tong, L. Du, G. K. So, F. F. Hung, T. L. Lam, G. Cheng, H. Xiao, X. Chang, Z. X. Xu and C. M. Che, Gold(I) Multi-resonance thermally activated delayed fluorescent emitters for highly efficient ultrapure-green organic light-emitting diodes, *Angew. Chem., Int. Ed.*, 2022, **61**, e202213392.

101 J. Wang, N. Li, C. Zhong, J. Miao, Z. Huang, M. Yu, Y. X. Hu, S. Luo, Y. Zou, K. Li and C. Yang, Metal-perturbed multiresonance TADF emitter enables high-efficiency and ultralow efficiency roll-off nonsensitized OLEDs with pure green gamut, *Adv. Mater.*, 2023, **35**, e2208378.

102 Y. Hu, J. Miao, C. Zhong, Y. Zeng, S. Gong, X. Cao, X. Zhou, Y. Gu and C. Yang, Peripherally heavy-atom-decorated strategy towards high-performance pure green electroluminescence with external quantum efficiency over 40%, *Angew. Chem., Int. Ed.*, 2023, **62**, e2023024.

103 F. Huang, Y.-C. Cheng, H. Wu, X. Xiong, J. Yu, X.-C. Fan, K. Wang and X.-H. Zhang, Hanging heavy atom-containing chains onto a multiple resonance framework: Influence on the TADF properties and device performances, *Chem. Eng. J.*, 2023, **465**, 142900.

104 F. Huang, X. C. Fan, Y. C. Cheng, Y. Xie, S. Luo, T. Zhang, H. Wu, X. Xiong, J. Yu, D. D. Zhang, X. K. Chen, K. Wang and X. H. Zhang, Multiple resonance organoboron OLED emitters with high efficiency and high color purity via managing long- and short-range charge-transfer excitations, *Adv. Opt. Mater.*, 2023, **11**, 2202950.

105 Y. Zhang, D. Zhang, J. Wei, X. Hong, Y. Lu, D. Hu, G. Li, Z. Liu, Y. Chen and L. Duan, Achieving pure green electroluminescence with CIEy of 0.69 and EQE of 28.2% from an aza-fused multi-resonance emitter, *Angew. Chem., Int. Ed.*, 2020, **59**, 17499.

106 X. F. Luo, H. X. Ni, H. L. Ma, Z. Z. Qu, J. Wang, Y. X. Zheng and J. L. Zuo, Fused π-extended multiple-resonance induced thermally activated delayed fluorescence materials for high-efficiency and narrowband OLEDs with low efficiency roll-off, *Adv. Opt. Mater.*, 2022, **10**, 2102513.

107 X. F. Luo, S. Q. Song, H. X. Ni, H. Ma, D. Yang, D. Ma, Y. X. Zheng and J. L. Zuo, Multiple-resonance-induced thermally activated delayed fluorescence materials based on indolo[3,2,1-*jk*]carbazole with an efficient narrowband pure-green electroluminescence, *Angew. Chem., Int. Ed.*, 2022, **61**, e202209984.

108 Y. Xu, Q. Wang, J. Wei, X. Peng, J. Xue, Z. Wang, S. J. Su and Y. Wang, Constructing organic electroluminescent material with very high color purity and efficiency based on polycyclization of the multiple resonance parent core, *Angew. Chem., Int. Ed.*, 2022, **61**, e202204652.

109 Q. Wang, Y. Xu, T. Huang, Y. Qu, J. Xue, B. Liang and Y. Wang, Precise regulation of emission maxima and construction of highly efficient electroluminescent materials with high color purity, *Angew. Chem., Int. Ed.*, 2023, **62**, e202301930.

110 J. Liu, Y. Zhu, T. Tsuboi, C. Deng, W. Lou, D. Wang, T. Liu and Q. Zhang, Toward a BT.2020 green emitter through a combined multiple resonance effect and multi-lock strategy, *Nat. Commun.*, 2022, **13**, 4876.

111 P. Jiang, L. Zhan, X. Cao, X. Lv, S. Gong, Z. Chen, C. Zhou, Z. Huang, F. Ni, Y. Zou and C. Yang, Simple acridan-based multi-resonance structures enable highly efficient narrowband green TADF electroluminescence, *Adv. Opt. Mater.*, 2021, **9**, 2100825.

112 G. Liu, H. Sasabe, K. Kumada, A. Matsunaga, H. Katagiri and J. Kido, Facile synthesis of multi-resonance ultra-pure-green TADF emitters based on bridged diarylamine derivatives for efficient OLEDs with narrow emission, *J. Mater. Chem. C*, 2021, **9**, 8308.

113 Y. X. Hu, J. Miao, T. Hua, Z. Huang, Y. Qi, Y. Zou, Y. Qiu, H. Xia, H. Liu, X. Cao and C. Yang, Efficient selenium-integrated TADF OLEDs with reduced roll-off, *Nat. Photonics*, 2022, **16**, 803.

114 F. Liu, Z. Cheng, Y. Jiang, L. Gao, H. Liu, H. Liu, Z. Feng, P. Lu and W. Yang, Highly efficient asymmetric multiple

resonance thermally activated delayed fluorescence emitter with EQE of 32.8% and extremely low efficiency roll-off, *Angew. Chem., Int. Ed.*, 2022, **61**, e202116927.

115 Y. Zhang, G. Li, L. Wang, T. Huang, J. Wei, G. Meng, X. Wang, X. Zeng, D. Zhang and L. Duan, Fusion of multi-resonance fragment with conventional polycyclic aromatic hydrocarbon for nearly BT.2020 green emission, *Angew. Chem., Int. Ed.*, 2022, **61**, e202202380.

116 X. Wu, J. W. Huang, B. K. Su, S. Wang, L. Yuan, W. Q. Zheng, H. Zhang, Y. X. Zheng, W. Zhu and P. T. Chou, Fabrication of circularly polarized MR-TADF emitters with asymmetrical peripheral-Lock enhancing helical B/N-doped nanographenes, *Adv. Mater.*, 2022, **34**, e2105080.

117 W. Yang, N. Li, J. Miao, L. Zhan, S. Gong, Z. Huang and C. Yang, Simple double hetero[5]helicenes realize highly efficient and narrowband circularly polarized organic light-emitting diodes, *CCS Chem.*, 2022, **4**, 3463.

118 Y. Yang, N. Li, J. Miao, X. Cao, A. Ying, K. Pan, X. Lv, F. Ni, Z. Huang, S. Gong and C. Yang, Chiral multi-resonance TADF emitters exhibiting narrowband circularly polarized electroluminescence with an EQE of 37.2%, *Angew. Chem., Int. Ed.*, 2022, **61**, e202202227.

119 N. Ikeda, S. Oda, R. Matsumoto, M. Yoshioka, D. Fukushima, K. Yoshiura, N. Yasuda and T. Hatakeyama, Solution-processable pure green thermally activated delayed fluorescence emitter based on the multiple resonance effect, *Adv. Mater.*, 2020, **32**, e2004072.

120 S. Oda, T. Sugitani, H. Tanaka, K. Tabata, R. Kawasumi and T. Hatakeyama, Development of pure green thermally activated delayed fluorescence material by cyano substitution, *Adv. Mater.*, 2022, **34**, e2201778.

121 S. Uemura, S. Oda, M. Hayakawa, R. Kawasumi, N. Ikeda, Y. T. Lee, C. Y. Chan, Y. Tsuchiya, C. Adachi and T. Hatakeyama, Sequential multiple borylation toward an ultrapure green thermally activated delayed fluorescence material, *J. Am. Chem. Soc.*, 2023, **145**, 1505.

122 X. Cai, J. Xue, C. Li, B. Liang, A. Ying, Y. Tan, S. Gong and Y. Wang, Achieving 37.1% green electroluminescent efficiency and 0.09 eV full width at half maximum based on a ternary boron-oxygen-nitrogen embedded polycyclic aromatic system, *Angew. Chem., Int. Ed.*, 2022, **61**, e202200337.

123 X. F. Luo, H. X. Ni, A. Q. Lv, X. K. Yao, H. L. Ma and Y. X. Zheng, High-efficiency and narrowband OLEDs from blue to yellow with ternary boron/nitrogen-based polycyclic heteroaromatic emitters, *Adv. Opt. Mater.*, 2022, **10**, 2200504.

124 Y. Zhang, D. Zhang, T. Huang, A. J. Gillett, Y. Liu, D. Hu, L. Cui, Z. Bin, G. Li, J. Wei and L. Duan, Multi-resonance deep-red emitters with shallow potential-energy surfaces to surpass energy-gap Law*, *Angew. Chem., Int. Ed.*, 2021, **60**, 20498.

125 Y. Wang, K. Zhang, F. Chen, X. Wang, Q. Yang, S. Wang, S. Shao and L. Wang, Boron-, sulfur- and nitrogen-doped tridecacyclic aromatic emitters with multiple resonance effect for narrowband red emission, *Chin. J. Chem.*, 2022, **40**, 2671.

126 Y. Zou, J. Hu, M. Yu, J. Miao, Z. Xie, Y. Qiu, X. Cao and C. Yang, High-performance narrowband pure-red OLEDs with external quantum efficiencies up to 36.1% and ultra-low efficiency roll-off, *Adv. Mater.*, 2022, **34**, e2201442.

127 T. Fan, M. Du, X. Jia, L. Wang, Z. Yin, Y. Shu, Y. Zhang, J. Wei, D. Zhang and L. Duan, High-efficiency narrowband multi-resonance emitter fusing indolocarbazole donors for BT. 2020 red electroluminescence and ultra-long operation lifetime, *Adv. Mater.*, 2023, 2301018.

128 Y. Liu, X. Xiao, Y. Ran, Z. Bin and J. You, Molecular design of thermally activated delayed fluorescent emitters for narrowband orange-red OLEDs boosted by a cyano-functionalization strategy, *Chem. Sci.*, 2021, **12**, 9408.

129 X. Cai, Y. Xu, Y. Pan, L. Li, Y. Pu, X. Zhuang, C. Li and Y. Wang, Solution-processable pure-red multiple resonance-induced thermally activated delayed fluorescence emitter for organic light-emitting diode with external quantum efficiency over 20%, *Angew. Chem., Int. Ed.*, 2023, **62**, e202216473.

130 Y. C. Cheng, X. C. Fan, F. Huang, X. Xiong, J. Yu, K. Wang, C. S. Lee and X. H. Zhang, A highly twisted carbazole-fused DABNA derivative as an orange-red TADF emitter for OLEDs with nearly 40% EQE, *Angew. Chem., Int. Ed.*, 2022, **61**, e202212575.

131 W. Yang, J. Miao, F. Hu, Y. Zou, C. Zhong, S. Gong and C. Yang, An effective approach toward yellow-to-orange multi-resonance TADF emitters by integrating strong electron donor into B/N-based polycyclic architecture: high performance OLEDs with nearly 40% EQE, *Adv. Funct. Mater.*, 2023, **33**, 2213056.